Chemical Characterization of the Boundary Layer Outflow of Air Pollution to Hong Kong during February- April 2001

Tao Wang[1], A. J. Ding[1,2], D. R. Blake[3], W. Zahorowski[4], C. N. Poon[1], and Y. S. Li[1]

[1] Department of Civil and Structural Engineering, The Hong Kong Polytechnic University, Hong Kong, China

[2] Department of Atmospheric Sciences, Nanjing University, Nanjing, China, 210093

[3] Department of Chemistry, University of California, Irvine, CA, 92697, U.S.A.

[4] Australian Nuclear Science and Technology Organization, Menai, New South Wales, Australia

Abstract. As a cooperative effort with the TRACE-P and ACE-Asia intensive in the spring of 2001, trace gases and aerosols were measured at a relatively remote coastal site (Hok Tsui) in southeastern Hong Kong. The main objective of the measurement program was to provide continuous ground-based data in the subtropical region of eastern Asia and to characterize the southward outflow of continental pollution that prevails in the lower atmosphere during early spring. In this paper, we present the results for ozone, CO, NO, NO_y, SO_2, ^{222}Radon, methane and C_2-C_8 non-methane hydrocarbons (NMHCs), C_1-C_2 halocarbons, and C_1-C_5 alkyl nitrate measurements obtained between February 19 and April 30, 2001. The average mixing ratios of O_3, CO, SO_2, and NO_y were 45 ppbv, 404 ppbv, 1.8 ppbv, and 10.4 ppbv, respectively. The two dominant NMHCs were ethane (mean: 2368 pptv) and ethyne (mean: 1402 pptv), followed by propane (814 pptv), toluene (540 pptv), benzene (492 pptv), ethene (498 pptv), and *n*-butane (326 pptv). The most abundant halocarbon was CH_3Cl (mean: 821

pptv), while 2-BuONO$_2$ and i-PrONO$_2$ were the two dominant alkyl nitrates species with a mean mixing ratio of 20 pptv and 19 pptv, respectively. The levels of trace gases were strongly influenced by the outflow of continental air masses initiated by the passage of cold fronts. The data are segregated into four air mass groups according to the levels of ^{222}Rn and wind direction, representing fresh continental outflow, coastal, perturbed maritime, and local urban air. Ozone and CO showed a moderate positive correlation (r^2=0.4) in the marine air group, characterized by low ^{222}Rn and CO levels, but they were poorly correlated in the other air mass groups. SO$_2$ and NO$_y$ exhibited good correlations ($r^2 > 0.6$) with each other but were poorly correlated with CO, indicating differences in their emission sources and/or removal processes. CO very strongly correlated with ethyne and benzene (r^2>0.85) and also showed good correlations with several other NMHCs. Moreover, CO correlated moderately with a biomass burning tracer (CH$_3$Cl) and an urban/industrial tracer (C$_2$Cl$_4$) indicating the impact of mixed pollution from urban and biomass burning sources. The relationship of CO, SO$_2$ and NO$_y$ with the indicator of atmospheric processing, ethyne/CO and propane/ethane, were also examined. The 2001 data were compared to the results obtained in the same period in 1994 during PEM-West B. The mean ozone level in the spring of 2001 was much higher than during PEM-West B. SO$_2$ also had higher concentrations during TRACE-P, while CO and NO$_y$ were comparable during the two campaigns. The observed difference has been discussed in the context of emission changes and variations in meteorology. Although it is difficult to draw definitive conclusions about the extent of the influence of these two factors, it appears that clearer

skies and drier conditions may have been responsible for the higher ozone concentrations during the TRACE-P period.

1. Introduction

Rapid industrialization has occurred in eastern Asia during the past two decades. The large demand for fossil fuels has led to a drastic rise in emissions of anthropogenic pollutants such as NO_x and SO_2 from 1980s to mid 1990s [*Akimoto and Narita*, 1994; *Van Aardenne et al.*, 1999; *Streets and Waldhoff*, 2000], and the emissions of SO_2 and NO_x are projected to continue increasing over the next 20 years [*van Aardenne et al.*, 1999]. However, Streets et al. [this issue] indicated that the economic downturn in Asia and re-structuring Chinese industrial economy in the late 1990s resulted in lower SO_2 and NO_x emissions than previously expected. Because of the potentially significant effects of Asian emissions on the chemistry and radiative balance over the Pacific region, it is crucial that the trend of emissions and the impacts are documented and characterized. In the past decade, a number of large-scale studies have been conducted to investigate the outflow of Asian air pollution to the western Pacific and regions further downwind, and the resulting impact on the environment [*Hoell et al*, 1996; *Hoell et al.*, 1997; *Crawford et al.*, 1997; *Elliot et al.*, 1997; *Jacob et al.*, 1999]. Many of the previous studies have focused on the eastward transport of the Asian outflow to the Pacific.

The Transport and Chemical Evolution over the Pacific (TRACE-P) [*Jacob et al.*, this issue] and the Aerosol Characterization Experiment – Asian Pacific region (ACE-Asia) [*Huebert et al.*, 2002] are two recent international endeavors conducted in

the spring of 2001, with the goal to better understand the chemistry, transport, and downwind impact of the outflow of Asian pollution. As a cooperative effort in support of the two international campaigns, we conducted measurements of a suite of trace gases and aerosols at a relatively remote coastal site in Hong Kong. The main objectives of our measurement program were to provide continuous ground-based data for the subtropical part of eastern Asia and to characterize the southward outflow of continental pollution prevailing in the boundary layer in early spring. Another objective of our study was to compare the recent observations during TRACE-P to the data collected at the same site during PEM-West B. *Wang et al.* [1997] presented the measurements of O_3, CO, SO_2 and NO_y for late February to March 1994. *Wang et al.* [2001] reported the results of measurements obtained in autumn (October-November) 1997. The multiple-year records of ozone and CO in 1994-1996 have been analyzed by *Lam et al.* [2001]. The long-term data indicate that the South China coast is strongly influenced by Asian monsoons that transport clean tropical air in the summer and polluted air masses from the Asian continent in the winter. The intensive measurement presented in Wang *et al.* [1997] reveals that the passage of cold fronts is an important mechanism for transporting continental pollution to the South China Sea during late winter and early spring. The previous studies also suggest a need for a more comprehensive measurement program to better characterize the boundary layer outflow which contain a complex mix of emissions.

In this study we report the measurement results of ozone, CO, NO, NO_y, SO_2,

^{222}Radon, methane, C_2-C_8 non-methane hydrocarbons (NMHCs), C_1-C_2 halocarbons, and C_1-C_5 alkyl nitrates obtained at Hok Tsui between February 19 and April 30, 2001. This time period covers the duration of the TRACE-P aircraft missions based in Hong Kong and Japan. The measurement results for the extended period for $PM_{2.5}$, PM_{10}, and Radon aerosols are separately presented by *Cohen et al.* [2002] and *Zahorowski et al.* [2002]. In this paper we first give an overview of the levels and variations of the measured trace gases, as well as of the major meteorological patterns affecting the variations in trace gases. The data are divided into several air mass groups based on the concentrations of ^{222}Rn and wind direction, representing fresh continental, coastal, and maritime, and local urban air masses transported to the site. Correlations of the trace species in each air mass group are compared in order to gain insight into photochemical production of ozone and emission source signatures. Finally, data for the year 2001 are compared to those obtained during PEM West B in 1994.

2. Experiment

2.1 The Hok Tsui study site

The measurements reported in this study were made at the atmospheric research station established by The Hong Kong Polytechnic University at Hok Tsui (Cape D'Aguilar), which is located in the southeastern tip of Hong Kong Island (22º13'N, 114º15'E, with an elevation of 60 m above sea level). A detailed description of the site and its surroundings is given in *Wang et al.* [1997; 2001]. Briefly, the site is in a relatively clean area of Hong Kong, situated on a cliff with 240 degrees of ocean view

stretching from northeast to southwest. Urban areas of Hong Kong are approximately 10 km from the site and are normally downwind under the prevailing east-northeast (E-NE) flow in spring.

Besides the urban areas of Hong Kong, other major emission sources within a 200-km radius from the site are concentrated in the Pearl River Delta (PRD) north and northwest of Hong Kong. The PRD is one of the most economically developed regions in China. By contrast, the area northeast of Hong Kong consists mostly of rural areas with relatively low levels of anthropogenic emissions [*Streets and Waldhoff*, 2000]. The island of Taiwan is about 600 km east of Hong Kong. Under the prevailing E-NE winds, the concentrations of trace constituents at the study site are expected to be largely determined by the transport of air masses from rural areas of southern China, the island of Taiwan, and the high-emission coastal regions of China. Occasionally, urban plumes from Hong Kong and the PRD can reach the site when winds are from the northwest and north. However, it should be noted that due to the close proximity of the site to the urban centers, emissions from these populated areas could affect the composition of "background" air sampled at the site even when the site was not directly downwind of the urban areas. In addition, as Hong Kong is a major hub of maritime transport, emissions from ships in and around Hong Kong waters can be an important source for species such as SO_2, NO_x, and black carbon.

2.2. Instrumental Methods

Ozone. O_3 was measured using a commercial UV photometric analyzer (Thermo

Environmental Instruments (TEI) Inc., Model 49C) with a detection limit of 2 ppbv (signal to noise ratio =2) and a precision of ±2 ppbv.

Carbon monoxide. CO was detected with an infrared gas filter correlation analyzer (TEI, Model 48). The analyzer had been modified to include a catalytic converter containing palladium heated to 250 °C (0.5% Pd on alumina, type E221 P/D catalyst, Deggussa Corp., Plainfield, New Jersey) for determining the instrument background. The detection limit (signal to noise ratio=2) was estimated to be ~18 ppbv for a 2-min integration time, and the precision (95% confidence) was approximately 20 ppbv for ambient levels of ~600 ppbv. The same instrument had been used during the PEM-West B study [*Wang et al.*, 1997].

Sulfur dioxide. SO_2 was measured by using a pulsed UV fluorescence analyzer (TEI, Model 43C). The detection limit for this analyzer is 0.06 ppbv for a 2-min integration with a precision of about 0.10 ppbv.

Nitric oxide (NO) and total reactive nitrogen (NO_y). NO and NO_y (NO_y = NO + NO_2 + HNO_3 + PAN + HONO+NO_3 + organic nitrate and aerosol nitrate…) was measured with a commercial chemiluminescence analyzer equipped with an externally placed Molybdenum oxide (MoO) catalytic converter (TEI, Model 42C-Y Trace Level). NO was detected using the chemiluminescent technique. NO_y was converted to NO on the surface of MoO at 350 °C, with NO subsequently measured by the chemilumenescent detector. The instrument automatically switched between the zero, NO, and NO_y modes. The analyzer had a detection limit of 0.05 ppbv. The 2-σ precision of this instrument was 4% (for NO=10 ppbv) and an uncertainty of about 10%.

The above real-time instruments were housed in a temperature-controlled laboratory. The O_3, CO and SO_2 analyzers shared a common sampling train: Ambient air was drawn at a height of 13 m above the ground through a PFA Teflon tube (outside diameter: 12.7 mm; inside diameter: 9.6 mm; length: 17.5 m) connected to a PFA manifold placed inside the laboratory. A bypass pump drew air at a rate of 15 liters per minute through the sampling manifold. The NO/NO_y detector used a separate sample line (inside diameter: 3.0 mm, length: 13.5 m) extending to a stainless steel enclosure placed at a height of 9 m above the ground. The enclosure housed the MoO converter and the calibration solenoid. The sample intake was a 15-cm long (inside diameter: 3.0 mm) PFA tubing prior to the converter. A bypass pump drew air samples constantly through the NO and NO_y sampling lines at a flow of 2 liters per minute to reduce the residence time in the sample line and to maintain air flow through the converter when the instrument was in NO mode. The sampling intakes for NO/NO_y and the rest of the gas analyzers were close to each other to ensure sample homogeneity. An in-line Teflon filter (Fluoroware Inc., Chaska, Minnesota) was placed upstream from each analyzer to prevent particles from entering into the analyzer.

These analyzers were calibrated on a daily basis by injecting a span gas mixture in scrubbed ambient air generated by a TEI model 111. A NIST traceable standard in an aluminum cylinder (Scott-Marrin Inc., California) containing 156.5 ppmv CO ($\pm$ 2%), 15.64 ppmv SO_2 ($\pm$ 2%), and 15.55 ppmv NO ($\pm$ 2%) was diluted using a dynamic calibrator (TEI, Model 146.). The NO_y conversion efficiency on MoO was checked using a 5-ppm N-propylnitrate (NPN) standard (Scott-Marrin, California) which was

used as the surrogate for NO_y [*Jaffe et al.*, 1996]. The conversion efficiencies of NPN were above 95% in the course of the study. Daily zero checks were also conducted. A data logger (Environmental Systems Corporation, model 8816) was used to control zero/span calibration and to collect 1-second data which was then averaged to 1-minute values. The data presented in this study are hourly averaged values.

^{222}Radon. Radon was measured with a dual-flow loop two-filter detector [*Whittlestone and Zahorowski*, 1998]. The detector at Hok Tsui was one of four radon detectors deployed in Southeast Asia and the Pacific Ocean to record hourly radon concentrations in air at selected ACE-Asia ground stations. The delay volume of the detector was 750 L and the corresponding lower limit of detection for a one-hour radon was count about 40 mBq m^{-3}. The response time, defined as the time needed to reach 50% of the maximum count rate after step increase in radon concentration, was about 45 minutes. Sample air was drawn continuously at a rate of 40 L/min from the top of an intake mast, 12 m above ground level (60m above sea level). Calibration of the detector was performed periodically by injecting radon from a radon source calibrated by the source's manufacturer (Pylon) against a NIST certified radium liquid standard.

Methane, NMHCs, halocarbons and alkyl-nitrates. Whole air samples were pressurized into 2-L evacuated stainless steel canisters using a metal bellows pump. The samples were taken mostly during 12:00-13:00 local time. Twenty-nine samples were obtained during March 3-April 26, 2001. More frequent samplings (~ daily) were conducted during the first two weeks covering the period of the TRACE-P aircraft transit flight to Hong Kong and local sorties. The canisters were then sent to the

University of California at Irvine (UCI) for chemical analysis. Details of the analytical procedures employed at the UCI laboratory for sample analysis can be found in *Sive* [1998], *Colman et al.* [2001] and *Blake et al.* [2002] and are outlined, as follows. For each sample 1285±2 cm^3 (STP) of air was preconcentrated in a liquid nitrogen-cooled loop filled with glass beads. After preconcentration the sample was directed to five different gas chromatographic column/detector combinations. Electron-capture detectors (ECD, sensitive to halocarbons and alkyl nitrates), flame-ionization detectors (FID, sensitive to hydrocarbons), and quadrupole mass spectrometers (MSD, for unambiguous compound identification and selected ion monitoring) were employed. CO was also quantified from the canister samples by first reducing CO to methane followed by gas chromatographic analyses with a FID detector. The analytical accuracy ranges from 2 to 20%. The precision of the measurements varies by compound and by mixing ratio. For example, the measurement precision is 2% or 3 pptv (whichever is larger) for the alkanes and alkynes, and 5% or 5 pptv (whichever is larger) for the alkenes [*Sive*, 1998]. The precision for the alkyl nitrates is about 4% [*Colman et al.*, 2001]. The precision for C_2Cl_4 at 5 pptv is ±0.1 pptv [*Colman et al.*, 2001]. The limit of detection (LOD) is 6 pptv for the NMHCs. The alkyl nitrate detection limit is 0.06 pptv [*Colman et al.*, 2001]. The CO result determined from canister samples was compared to time-matched real-time analyzer data, showing an agreement within 10% ([CO]$_{canister}$ = 0.91 * [CO]$_{TEI}$ − 4.7, r^2=0.90).

3. Results and Discussions

3.1 Weather conditions in spring

The main synoptic features for eastern Asia in spring can be summarized as follows [see also *Ding*, 1994; *Fuelberg et al.*, this issue; *Bey et al.*, 2001]: Spring is the transitional period between the winter and summer monsoons. In late winter the Siberian High produces strong northeasterly winds in the boundary layer along the Pacific Rim. The meteorological situation in southeastern China is also characterized by frequent passages of cold fronts moving southwards from northern China. By March, the Siberian High weakens, while the Pacific High is building up. As a result, the strength of the winter monsoon winds and the frequency of the cold fronts decrease, while the intrusions of warmer tropical air from the South become more frequent. These synoptic features are illustrated in Figure 1a-c, showing the mean geopotential height and streamline at 1000hPa for February 19–April 30, 2001, a case of cold surge (on February 28) and a case of maritime air inflow (on April 29), respectively. The plots were made using NCEP/NCAR reanalysis data available at the following website: http://ww.cdc.noaa.gov/cdc/data.necp.reanalysis.html. As will be shown below, the alternations of these synoptic patterns strongly influenced day-to-day variations in surface winds and, consequently, the levels of trace gases (and aerosols) measured at the site. During February 21-April 30, 2001, there were ten cold surges while inflows of marine air were observed on only four occasions. All of the marine inflow events occurred in the second half of the study.

3.2. Overall results during TRACE-P

Figure 2 shows the temporal variations of trace gases measured at Hok Tsui and

surface winds recorded at Waglan Island about 5 km southeast of Hok Tsui. The dates

for the TRACE-P flights near Hong Kong, the passage of cold fronts and inflows of

marine air are also marked. There were large day-to-day variations in the trace gas

levels. The concentrations of ^{222}Rn and other gases showed significant enhancements

when the winds switched from prevailing E-NE to north-northwest (N-NW) (e.g.,

February 28), indicating the impact of emissions from adjacent lands (for ^{222}Rn) and

from major urban areas in the N-NW directions. Examination of aerosol data [*Cohen et

al.*, 2002] also indicated high sulfate concentrations when the winds shifted north. Two

moderately strong dust storms transported from northern China were observed on

March 9 and April 12-13, during which the trace gases did not show unusual changes

(see Figure 2). For example, CO - which is a tracer of combustion sources - maintained

a consistent level of 300-400 ppbv during the dust events. In general, CO and ^{222}Rn

closely tracked each other, while SO_2 and NO_y showed larger variations. Moderately

high ozone levels were observed with a daytime peak in the range of 60-80 ppbv. On

several occasions (March 24-25, April 8, 21, and 30), much lower levels of ^{222}Rn, CO

and O_3 were observed with winds from the south and southwest. An examination of

synoptic weather charts shows that the N-NW winds were associated with the passage

of a cold front and/or the onset of the winter monsoon, initiating the outflow of

continental pollution. By contrast, the reduced levels observed in the south southwest

(S-SW) were due to the inflow of maritime air. Most of the time, winds were from the

NE, with moderate concentrations of trace gas characteristic of 'aged' continental air.

Table 1 lists the major synoptic weather patterns that have affected trace gas levels.

Table 2 summarizes the statistics of O_3, CO, NO, NO_y, SO_2, methane and major

NMHCs, halocarbons and alkyl nitrates. The average CO, NO_y and SO_2 levels at this

South China site are approximately twice or more of the concentrations in "polluted"

rural atmospheres in the eastern United States [e.g., *Parrish et al.*, 1991; *Parrish et al.*,

1993], while the O_3 level is comparable. Ethane (mean: 2368 pptv) and ethyne (mean:

1402 pptv) are the two most abundant NMHC compounds, followed by propane (814

pptv), toluene (540 pptv), ethene (498 pptv), benzene (492 pptv), and *n*-butane (326

pptv). The most abundant halocarbon is CH_3Cl (821 pptv) while *2*-BuONO$_2$ and

i-ProONO$_2$ are the two dominant alkyl nitrates species with a mean mixing ratio of 20

pptv and 19 pptv, respectively. These concentrations were compared with the results

obtained on the TRACE-P aircraft in locations downwind of the Asian outflow. *Russo*

et al. [this issue] examined the chemical composition of air mass originated from

different source regions including the central (30-60ºN, 80-130ºE) and coastal

(20-40ºN, 90-130ºE) regions. Compared to the data from the central region for altitudes

below 2 km, which included the highly polluted Shanghai plume, our surface

measurements had comparable C_2H_2 and C_6H_6, more abundant NO_y, C_2Cl_4, and CH_3Cl,

but lower O_3, SO_2, C_2H_6 and C_3H_8. Compared to the aircraft data from the coastal

region, the ground-based result indicated higher mixing ratios for most of the measured

species. This can be attributed in part to the closer proximity of our sampling site to

source regions on the continent as well as in the Hong Kong area.

3.3. Classification of air masses using ^{222}Rn

To compare the chemical characteristics of air masses from different regions or

with different histories of atmospheric processing, it is important to segregate the bulk data into groups. Back trajectory is an approach that has been widely used to track the path, origin, and transit time by an air mass. An alternative classification scheme uses certain chemical species or ratios such as C_2H_2/CO and C_3H_8/C_2H_6 [e.g., *Smyth et al.*, 1999]. Our previous studies [*Wang et al.*, 1997; 2001] showed that the application of trajectories based on coarse-resolution (1°x1°) meteorological data could be complicated by rapid change of winds (e.g., land-sea breezes) that were not captured by the trajectories, calculated twice a day. The use of the C_2H_2/CO is limited by relatively small numbers of canister samples (N=29). It is thus desirable to use a chemical species that was measured on a continuous basis.

We attempt to use ^{222}Radon to identify air masses originating from continental boundary layers. ^{222}Rn comes from the radioactive decay of uranium which is present in rocks, soil and earth, but not in water. The oceanic flux is two or three orders of magnitude less than the land flux. Radon is not lost from the atmosphere by chemical reactions or deposition. Its only atmospheric sink is the radioactive decay with a half-life time of 3.8 days, which is similar to many atmospheric trace gases (i.e., NO_x and C_2H_4). For these reasons ^{222}Rn has been used to aid the interpretation of measurements of other atmospheric trace species [*Whittlesone et al.*, 1985; *Larson et al.*, 1972; *Wilknis et al.*, 1974]. Figure 3 shows the scatter plot of ^{222}Rn and CO, a tracer of the anthropogenic (combustion) pollution. As expected, the two species showed a good positive correlation (r^2 =0.56). An examination of the time series indicates that ^{222}Rn exhibited a more gradual decline than did CO after the passage of fresh

continental air. Figure 4 shows such an example. This suggests that ^{222}Rn is more representative of air masses that have had recent contact with land, whereas the variation of CO is more strongly impacted by combustion pollution (i.e., urban plumes from the PRD) in the initial stage of the outflow.

We divided the data into four groups based on the values of the natural logarithm of ^{222}Rn concentrations and wind direction. Data with lnRn less than the mean, minus half of standard deviation, are considered to have been less impacted by the continent and are assigned as having a maritime origin (Type M) whereas data with a lnRn$\geq$ mean, plus half standard deviation, are representative of fresh continental outflow (Type C), after excluding the data associated with wind directions 270°-10° which were separately classified to Type C-U to represent local urban pollution. Measurements falling in between the Type C and M, (i.e., mean-0.5Std. Dev.$\leq ln$Rn < mean+0.5Std. Dev.) are assigned to the coastal group (Type C-M). The selection of 0.5 standard deviation was based on the results of a series of trials using a factor 0.2x with an increment of 0.1 for each test. It appears that the use of 0.5 captured outflow of continental air, indicated by the highest levels of ^{222}Rn and CO and the cases for the intrusion of clean maritime air. Figure 5 shows the frequency distribution of wind direction for the four air-mass types, which is consistent with the contention that the "marine" air is mostly associated with easterly and southerly winds while the fresh continental outflow predominantly comes from the north and northeast. The percentage of each group is 23% (Type M), 18% (Type C), 50% (Type C-M), and 9% (Type C-U), respectively. There was one case (on March 21) in the urban plume group showing high

^{222}Rn with southerly winds, which was due to the re-circulation of urban air by land-sea breezes. Our discussion below focuses on Type M, C and C-M as they are thought to be less affected by local urban emissions. Nevertheless, the data in the urban group (Type C-U) are used in some plots to contrast correlations in the above three groups to the emission ratios of local urban pollution.

Table 3 summarizes the statistics for the principle species of each air mass type. Most anthropogenic species (CO, NMHC, and halocarbons) had the highest concentrations of fresh continental outflow (Type C). (As expected, the highest levels are found in urban plumes from Hong Kong and the PRD). The marine group (M) contains the lowest concentrations of most of the trace gases, with the coastal group in the middle. An exception is for NO, NO_y, SO_2, whose concentrations are in fact higher in the marine group than, or comparable to, those in the coastal group (Type C-M). This appears to be due to the emissions of ships in the heavily trafficked coastal waters of the South China Sea. Moreover, the NO to NO_y ratio for the type M (0.17) is higher than for the coastal group (0.08) and for the continental group (0.14). The large NO fraction in NO_y suggests that the NO had not have time to be fully converted to NO_y upon sampling, suggesting that near-field ship emissions were likely the principal source for NO_y and SO_2 in the marine group. The higher CH_3Br and CH_3I levels in the coastal and marine group reflect contributions from oceanic sources. Concerning O_3, the coastal group has the highest mean value (53 ppbv), followed by the fresh outflow group (42 ppbv), the marine group (38 ppbv), and the fresh urban plume (23 ppbv).

The values of C_3H_8/C_2H_6 and C_2H_2/CO have been used as a measure of

atmospheric processing (dynamic mixing and chemical reactions) in an air mass after a recent injection of anthropogenic pollutants [e.g., *Smyth et al.*, 1999]. Table 3 shows that the mean C_3H_8/C_2H_6 ranges from 0.37 (ppbv/ppbv) in the fresh continental outflow group to 0.25 ppbv in the marine group. The decreasing ratio can be explained in part by the faster removal of C_3H_8 via reaction with OH radicals. *Russo et al.* [this issue] obtained a mean ratio of 0.35 and 0.19 ppbv/ppbv from the "Central" and "Coastal" source regions. For C_2H_2/CO, the mean values observed at our site is 4.3 (pptv/ppbv), 3.8, and 3.2 for type C, C-M, and M, respectively. *Russo et al.* [this issue] observed an average ratio of 3.87 and 2.46 in "Central" and "Coastal" airmass group, respectively. The above results indicate that the data segregation using the radon data are consistent with the use of the two chemical indicators, C_3H_8/C_2H_6 and C_2H_2/CO.

3.4. Interspecies correlations

Ozone versus CO: Ozone produced from anthropogenic precursors has been found to show a positive correlation with CO, an important tracer of urban pollution [e.g., *Parrish et al.*, 1998, *Wang et al.*, 2001]. Figure 6 shows scatter plots of O_3 and CO for the different air mass groups observed in Hok Tsui. A moderately good positive correlation ($r^2=0.40$) is indicated in the marine group with a slope of 0.18, while there is either a lack of correlation or a weak negative correlation in Type C and Type C-M with the urban group having a similar result (not shown). A positive O_3-CO correlation is expected in an air mass that has a large loading of anthropogenic emissions experiencing strong photochemical processing which leads to the formation of ozone. The O_3-CO correlation shown in Figure 6 suggests that the ozone was produced in aged

air masses that had reduced CO levels, whereas the outflow of a fresh continental air mass suppressed the ozone formation due to an overabundance of NO_x and the titration of peroxy radicals. The slope for the marine group in our study is somewhat smaller than those observed in the outflow of pollution from the northeastern United States to the North Atlantic Ocean [*Parrish et al.*, 1998]. Based on measurements at several ground stations off the coast of Nova Scotia, they found that the O_3-CO slopes ranged from 0.25 to 0.42 in warm seasons (May-September). The smaller slope observed at the present site may be attributed to a reduced efficiency in photochemical production in the spring or to a larger emission ratio of CO to NO_x in China. *Wang et al.*, [2001] reported a summertime O_3-CO slope of 0.1 observed at a rural site, Lin'an, in eastern China, owing to very high CO to NO_x ratios at that site.

O_3 versus NO_y: A positive O_3-NO_y correlation has been observed in rural and maritime locations downwind of major urban and industrial sources [e.g., *Trainer et al.*, 1993; *Buhr et al.*, 1996; *Wang et al.*, 2001]. Figure 7 shows a scatter plot of O_3 and NO_y for the marine, coastal and continental groups. An overall negative correlation is indicated, which is similar to our previous result obtained during PEM-West B at this site. The lack of positive correlation in Type C can be attributed to both the titration and suppression of ozone formation in the fresh continental outflow, whereas a negative correlation in the marine group can be explained by the different time histories of ozone and NOy. That is, the measured ozone in the Type M was produced over the ocean during transport to Hong Kong while NOy was injected into the air mass from ships near the Hong Kong area.

O$_3$ versus sum of (> C$_2$) alkyl nitrates: O$_3$ and sum of (>C$_2$) alkyl nitrates are also expected to be positively correlated in 'aged' air masses because both are products of atmospheric photochemistry involving NO$_x$ [e.g., *Robert et al.*, 1998]. However, such a relationship was not strongly indicated at our site (Figure 8a). (The plot includes all data without dividing them into air-mass groups due to limited number of canister samples.) This observation, which is consistent with other evidence found in the study, implies the mixing of air masses with different photochemical histories and/or different emission signatures. By comparison, CO and alkyl nitrates are slightly better correlated, as shown in Figure 8b.

CO versus NO$_y$ and SO$_2$: The relationships of these three species can reveal valuable insights into their emission sources and their removals during transport. Figure 9 shows positive correlations between SO$_2$ and NO$_y$, with r^2 ranging from 0.44-0.74 for all the four air-mass groups. There is a noticeable difference in the slopes for the different air-mass groups. The urban plumes give a slope of 0.1 compared to 0.13-0.21 in other air-mass groups. The slope in the urban plume is very close to the ratio observed in the urban atmosphere of Hong Kong, suggesting that Hong Kong's emissions have a significant impact on this category of air mass. By comparison, the slope of ~0.2 can be considered typical of emissions from rural areas of South China and/or from ships in the South China Sea. The strongest correlation was found in the coastal and maritime groups. The relatively low SO$_2$ to NO$_y$ ratio observed in the south China site contrasts with the large ratio (~1.0 ppbv/ppbv) found at Lin'an in eastern China [*Wang et al.*, 2002], reflecting a difference in emission characteristics in the

southern and eastern part of China. Although the majority of data for Hok Tsui have low SO_2/NO_y, there are a group of points in Figure 9 with moderate SO_2 mixing ratios (~2.5 ppbv) and a SO_2/NO_y of ~0.5. An examination of SO_2/NO_y as a function of wind direction reveals that the high SO_2/NO_y values are mostly associated with winds from the east to northeast, suggesting the transport of SO_2-rich air masses from outside of Hong Kong.

In contrast to a strong SO_2-NO_y correlation, a weak relationship is found for CO and NO_y except in urban plumes (r^2=0.48) (see Figure 10). A similar trend was observed during PEM-West B [*Wang et al.*, 1997]. The weak CO-NO_y correlation in non-urban plumes is attributed to the removal of NO_y (by precipitation scavenge and dry deposition) in aged air masses and to much larger emission ratios of NO_y to CO from ships.

CO versus NMHCs and halocarbons: CO is emitted primarily from the incomplete combustion of fossil fuel and the burning of vegetation. The sources for CO also emit some NMHCs and halocarbons (e.g., ethyne from vehicle exhaust) or co-locate with emission sources of halocarbons. An examination of the relationship of CO with NMHCs and halocarbons can thus provide useful information on their sources and emission signatures. Figure 11 shows scatter plots of CO and selected NMHCs and halocarbons. These plots are based on all 29 samples collected during the study period. (Plotting the data for different air-mass groups gave an expected result, i.e., the data in the marine group are mostly in the low-value regime and those in the continental group tend to have higher values.)   It can be seen that among the NMHCs measured, ethyne

was best correlated with CO (slope=5.3 pptv/ppbv, r^2=0.93), confirming their common source origin. This ratio is significantly larger than that reported by *Golden et al.* [2000], C_2H_2/CO of 2.1 pptv/ppbv, based on airborne results during the SOS 1995 Nashville Study, suggesting the freshness of air sampled at the Hok Tsui site. Benzene also showed a strong correlation with CO (r^2=0.74) at Hok Tsui. Similarly, alkanes and alkenes were positively correlated with CO (r^2=0.60 for C_2H_6, 0.59 for C_3H_8, 0.46 for C_2H_4).

Methyl chloride (CH_3Cl) has been used as a tracer for biomass burning [*Blake et al.*, 1996] while C_2Cl_4 is exclusively released by urban/industrial processes [*Wang et al.*, 1995]. Figure 11 shows that these two species are moderately correlated with CO, indicating that observed CO was from both urban pollution and biomass burning. We also examined the scatter plots of SO_2 and NO_y with C_2Cl_4 and CH_3Cl (Figure not shown), and no clear relationship was found. This is consistent with a lack of correlation of SO_2 and NO_y with CO, suggesting that the SO_2 and NO_y at Hok Tsui largely come from emission sources different from those for CO. *Talbot et al.* [this issue] also found poor relationships between NO_y and the two tracers in the TRACE-P airborne data.

Relations to C_2H_2/CO and Propane/ethane: As previously mentioned, C_2H_2/CO and C_3H_8/C_2H_6 can serve as a measure of atmospheric processing in an air mass. Figure 12 shows the scatter plots of O_3, CO, SO_2, NO_y. It can be seen that while CO had some correlation with the C_2H_2/CO and C_3H_8/C_2H_6 ratios, O_3, NO_y and SO_2 had no relationships. This result, which is consistent with other evidence found in this study,

suggests that the CO measured at the site was not related to the sources that emitted the observed NO_y and SO_2, and that the O_3 variation was influenced by both long-range transport and sub-regional emissions.

3.6. Comparison to PEM-WEST B

It is of great interest to compare the spring 2001 data to the results obtained in same period in 1994 to learn about the possible signal of emission changes over the 7-year span. *Wang et al.* [1997] presented O_3, CO, SO_2 and NO_y measured at the same site during February 18 to March 14, 1994. Table 4 summarizes mean, median, 90th and 10th percentiles of the mixing ratios for these species obtained during the two field campaigns. Figure 13 shows the frequency distributions. It can be seen that some gases have similar levels during the two studies while others show a different abundance. The O_3 levels were much higher in 2001 than in 1994 (median: 48 ppbv versus 34 ppbv). The median SO_2 observed was also higher during TRACE-P compared to PEM-West B (1.43 versus 0.95 ppbv). By contrast, CO and NO_y were comparable during TRACE-P and PEM-West B. The median CO mixing ratio was 437 ppbv in TRACE-P compared to 462 ppbv during PEM-WEST B; NO_y was 7.25 ppbv for TRACE-P and PEM-West B.

Russo et al. [this issue] compared aircraft data obtained during TRACE-P and PEM West B. Throughout the western Pacific, ozone was enhanced by 10-20 ppbv increase during TRACE-P for air coming from latitudes north of 20 degrees. NO_y also exhibited significant enhancements during TRACE-P in the boundary layer of the northern latitudes. Higher SO_2 was observed in the boundary layer. CO was similar in the two

missions although slightly higher levels were encountered in the boundary layer during TRACE-P.

The atmospheric abundance of a trace gas is determined by emission strength as well as by atmospheric processes that transform, produce, dilute, and remove the species of interest. Concerning the emission trend, *Streets et al.* [this issue] showed that the SO_2 emission in China had decreased by 16% from 1994 to 2000 while NO_x had increased by 10%. No quantitative comparison of the CO trend was given due to a lack of CO emission data for 1994, but it is believed that emissions of CO have been quite stable [*Streets et al.*, this issue]. Their estimate of a reduction in SO_2 emissions is consistent with the official estimate of the Chinese government suggesting a decrease of 16% at the national level from 1995 to 2000 [*People's Republic of China Yearbook*, 2001]. It should be noted that, although SO_2 emissions at the national levels have overall declined, the southern regions of China may have emission trends different from those of northern provinces. In Guangdong, which is the province that borders Hong Kong, SO_2 emissions have in fact increased by 20% between 1995 and 2000 [*Guangdong Statistical Yearbook*, 2001]. The overall increase is due to a sharp jump in emissions in 2000.

Besides emission trends, changes in meteorological conditions can also have a large impact on the year-to-year variations in the distribution of trace gases. A comparison of the synoptic weather charts during the PEM-West B and TRACE-P periods showed that the high-pressure system over the Asian continent appeared to extend to the southeast part of China during TRACE-P, whereas it stayed in more

northerly locations during PEM-WEST B (see Figure 14). Meteorological conditions recorded in Hong Kong also reveal differences for the two field campaigns. Overall, the spring 2001 study was conducted in a drier and sunnier period with slightly higher temperatures (Table 5). The average relative humidity in Hong Kong was 77% during the recent study, compared to 84% for the 1994 campaign. The precipitation was 6 mm versus 15 mm; the mean amount of sunshine was 5.1 hours versus 1.8 hours; and the mean surface temperature was 17.9 °C versus 15.3 °C. Surface winds also showed an increased frequency of easterly components, as shown in Figure 15.

The above differences in meteorological conditions can explain, at least in part, the increase in surface ozone observed at the Hong Kong site. The greater amounts of sunlight and the higher temperatures would enhance photochemical formation of O_3, and less rainfall would reduce the scavenging of free radicals involved in ozone production. The more frequent easterly winds would bring in air masses that were less affected by fresh urban pollution. For SO_2, the increased emissions in Guangdong and possibly in other southern provinces of China could be a partial cause of its higher levels, but the drier conditions in spring 2001 could have reduced the removal of SO_2, which would also explain its higher concentrations. It is difficult to conclude how much of the observed difference is emission-driven or due to changes in meteorological conditions. *Liu et al.* [this issue] found a much greater frequency of cold frontal passages across eastern Asia during TRACE-P than during PEM-West B, contributing to a stronger boundary layer outflow of continental pollution to the western Pacific. Clearly, more studies are needed to explain the difference/similarity of trace gases at the

Hok Tsui site.

4. Summary and conclusions

We have presented the measurement of a suite of trace gases obtained in spring of 2001 at a coastal site in Hong Kong (Hok Tsui). The aim of this study was to determine the chemical composition of the strong southward boundary layer outflow of continental pollution to the South China Sea region. The levels of the measured trace gases were strongly influenced by the outflow of continental air masses initiated by the passage of cold fronts. The average mixing ratio of O_3, CO, SO_2, and NO_y was 45 ppbv, 404 ppbv, 1.8 ppbv, and 10.4 ppbv, respectively. The dominant NMHCs were ethane (mean: 2368 pptv), ethyne (mean: 1402 pptv), propane (814 pptv), toluene (540 pptv), ethene (498 pptv), benzene (492 pptv), and n-butane (326 pptv). The most abundant halocarbon was CH_3Cl (mean: 821 pptv) while 2-BuONO$_2$ (20 pptv) and i-ProONO$_2$ (19 pptv) were the two dominant C_1-C_5 alkyl nitrates species. The moderate correlation between ozone and CO in 'aged' air masses implies ozone production during transport to Hong Kong while ozone in fresh outflow was suppressed by chemical titration. The strong positive correlation between SO_2 and NO_y suggests that they originate from common or co-located sources, and emissions from ships in the coastal waters of Hong Kong appear to be an important source. CO showed a poor correlation with SO_2 and NO_y except in urban plumes, but strongly correlated with most of the measured NMHCs, particularly ethyne and benzene. CO also showed moderate correlations with an urban/industrial tracer, C_2Cl_4, and a biomass burning tracer, CH_3Cl, implying

contributions from both urban pollution and biomass burning to the air masses sampled during the study period. An analysis of aerosol data [Cohen et. al, 2002] indicated some evidence of the long-range transport of dust from northern China to Hong Kong during the study period. Higher O_3 concentrations were found in 2001 during the same period (February 19-March 13) in 1994. SO_2 also showed higher levels in the recent measurement, while CO and NO_y were comparable during the two campaigns. It appears that the increase in ozone is attributable in part to the drier and sunnier conditions of the 2001 study. It is more difficult to come to a conclusion about the relative contributions of changes in emissions and/or meteorology in explaining the similarities and differences among SO_2, NO_y and CO observed during the two studies.

The study reveals that air masses arriving at the site contain mixed chemical signatures from urban pollution, biomass burning, ship exhaust, and occasionally dust. Local and sub-regional sources of emissions are superimposed on the large-scale continental outflow. Further studies are needed to quantify the relative contributions from the various sources and to investigate what impact the strong springtime boundary outflow of pollution has on the chemistry and radiative budget of the subtropical part of eastern Asia. The measurements have shown that ships may be an important source for SO_2 and NO_y in the coastal areas and possibly the South China Sea region. Detailed studies of the implications of ship emissions on the ozone budget and the formation of condensation nuclei in the marine boundary layer are needed.

Acknowledgments

References

Akimoto, H. and Hirohito Narita, Distribution of SO_2, NO_x and CO_2 emissions from fuel combustion and industrial activities in Asia with $1^o \times 1^o$ resolution, *Atmospheric Environment* Vol.28, No.2, p.213-225, 1994.

Bey, I. et al., Asian chemical outflow to the Pacific in spring: origins, pathways, and budgets. *J. Geophys. Res*., 106, 23,097-23,144, 2001.

Blake, N.J., D. R. Blake, B. C. Sive, T-Y. Chen, F. S. Rowland, J. E. Collins Jr, G. W. Sachse, and B. E. Anderson, Biomass burning emissions and vertical distribution of atmospheric methyl halides and other reduced carbon gases in the South Atlantic Region, *J. Geophys. Res.,* 101, 24,141-24,164, 1996.

Blake, N.J., D.R. Blake, A.L. Swanson, E. Atlas, F. Flock and F. S. Rowland, Latitudinal, vertical and seasonal variations in C_1-C_4 alkyl nitrates in the troposphere over the Pacific Ocean during PEM-Tropics A and B: Oceanic and continental sources, *J. Geophys. Res.*, in press, 2002.

Buhr, M.P., D. Sueper, M. Trainer, P. Goldan, B. Kuster, F. Fehsenfeld, G. Kok, R. Shillawski, and Allan Schanot, Trace gas and aerosol measurements using aircraft data from the North Atlantic Regional Experiment (NARE 1993).*J. Geophys. Res.* 101(D22), 29,013-29,027, 1996.

Cohen D.D. et al., Multi-elemental analysis and characterization of fine aerosols at several key ACE-Asia sites, submitted to *J. Geophys. Res.,* 2002.

Colman J.J., A. L. Swanson, S. Meinardi, B. C. Sive, D. R. Blake and F. S. Rowland, Description of the analysis of a wide range of volatile organic compounds in

whole air samples collected during PEM-Tropics A and B, *Analytical Chemistry*, 73(N15), 3723-3731, 2001.

Crawford, J. H., et al., An assessment of ozone photochemistry in the extratropical western North Pacific: Impact of continental outflow during the late winter/early spring. *J. Geophys. Res.*, 102(D23), 28,469-28,488, 1997

Ding Yihui, Monsoons over China, *Kluwer Academic Publishers,* 1994

Elliott, S., D. R. Blake, R. A. Ruce, C. A. Lai, I. McCreary, L.A. McNair, F.S. Rowland, and A.G. Russell, Motorization of China implies changes in Pacific air chemistry and primary production, *Geophys. Res. Lett.*, 24, 2671-2674, 1997.

Fuelberg, H.E., C.M. Kiley, J. R. Hannan, D.J. Westberg, M.A. Avery, and R.E. Newell, Atmospheric transport during the Transport and Chemical Evolution over the Pacific (TRACE-P) experiment, *J. Geophys. Res.,* this issue.

Golden, P.D., D. D. Parrish, W. C. Kuster, and M. Trainer, S. A. McKeen, J. Holloway, B. T. Jobson, and D. T. Sueper, F. C. Fehsenfeld, Airborne measurements of isoprene, CO and anthropogenic hydrocarbons and their implications, *J. Geophys. Res.,* 105(D7), 9091-9105, 2000.

Guangdong Statistical Yearbook, 2001, *China Statistics Press*, Beijing, August 2001.

Hoell, J. M., D. D. Davis, S.C. Liu, R. Newell, M. Shipham, H. Akimoto, R.J. McNeal, R.J. Bendura, and J.W. Drewry, The Pacific Exploratory Mission-West A (PEM-West A): September-October, 1991, *J. Geophys. Res.*, *101*, 1641-1653, 1996.

Hoell, J.M., Davis, D.D., Liu, S.C., Newell, R.E., Akimoto, H., McNeal, R.J., Bendura,

R.J., The Pacific exploratory mission west phase B: February–March 1994. *J. Geophys. Res.* 102, 28,223–28,239, 1997

Huebert, B., T. Bates, P. Russell, J. Seinfeld, M. Wang, M. Uematsu, and Y.J. Kim, An overview of ACE-Asia: strategies for quantifying the relationships between Asian aerosols and their climatic impacts, submitted to *J. Geophys. Res.*, 2002.

Jacob, D. J., A. Logan, and P. P. Murti, Effects of rising Asian emissions on surface ozone in the United State, *Geophys. Res. Lett.*, 26, 2175-2178, 1999.

Jacob, D.J. et al., The Transport and Chemical Evolution over the Pacific (TRACE-P) mission: design, execution, and overview of results, *J. Geophys. Res.* (this issue)

Jaffe, D.A et al. Measurement of NO, NO_y, CO and O_3 and estimation of the ozone production rate at Oki Island, Japan, during PEM-West. *J. Geophys. Res.* 101(D7), 2037-2048, 1996.

Lam, K.S., T. J. Wang, L. Y. Chan, T. Wang and J. Harris. Flow patterns influencing the seasonal behavior of surface ozone and carbon monoxide at a coastal site near Hong Kong, *Atmospheric Environment*, 35, 3121-3135, 2001

Larson, R. E., Lamontagne, R. A., and Wilkniss, P. E.. Radon-222, CO, CH_4 and continental dust over the Greenland and Norwegian Seas. *Nature*, 240: 345-347,1972

Liu Hongyu, et al., Transport pathways for Asian combustion outflow over the pacific: Interannual and seasonal variations, *J. Geophys. Res.*, this issue.

Parrish D.D., M. Trainer, M.P. Buhr, B. A. Watkins, and F.C. Fehsenfeld, Carbon monoxide concentrations and their relation to concentrations of total reactive

oxidized nitrogen at two rural U.S. sites, *J. Geophys. Res.*, 96, 9309-9320, 1991.

Parrish, D.D., et al., The total reactive oxidized nitrogen levels and their partitioning between the individual species at six rural sites in eastern North America. *J. Geophys. Res.*, 98-2927-2939, 1993.

Parrish, D. D., M. Trainer, J. S. Holloway, J. E. Yee, M. S. Warshawsky, and F. C. Fehsenfeld, Relationships between ozone and carbon monoxide at surface sites in the North Atlantic region, *J. Geophys. Res.*, 103(D11), 13,357-13,376, 1998.

Roberts, J.M, S. B .Bertman, D. D. Parrish, F.C. Fehsenfeld, B. T. Jobson, and H. Niki, Measurement of alkyl nitrates at Chebogue Point, Nova Scotia during the 1993 North Atlantic Regional Experiment (NARE) intersive, *J.Geophy. Res.*, 103(D11), 13,569-13,580, 1998.

Russo. R, R. Talbot, J. Dibb, E. Scheuer, G. Seid, S. Sandholm, D. Tan, H. Singh, D. Blake, N. Blake, E. Atlas, C. Jordan, G. Sachse, M. Avery, S. Vay, J. Snow, B. Heikes, Chemical composition of Asian continental outflow over the western Pacific: Results from TRACE-P, *J. Geophys. Res.*, this issue.

Sive, B. C. PH.D. Dissertation, University of California, Irvine, 1998.

Smyth, S., S. Sandholm, B. Schumaker, W. Mitch, A. Kanvinde, J. Bradshaw, S. Liu, S. McKeen, G. Greogory, B. Anderson, R. Talbot, D. Blake, S. Rowland, E. Browell, M. Fenn, J. Merrill, S. Bachmeier, G. Sachse, and J. Collins, Characterization of the chemical signatures of air masses observed during the PEM experiments over the western Pacific, *J. Geophys. Res., 104*, 16,243-16,254, 1999.

Streets, D.G. and Waldhoff, S.T., Present and future emissions of air pollutants in

China: SO_2, NO_x, and CO. *Atmospheric Environment* Vol.34, p363-374, 2000.

Streets, D.G., et al., An inventory of gaseous and primary aerosol emissions in Asia in the year 2000, *J. Geophys. Res.,* this issue.

Talbot, R.W., et al., Chemical characteristics of continent outflow from Asia to the troposphere over the western Pacific Ocean during February-March 1994: Results from PEM-West B. *J. Geophys. Res.*, 102 (D23), 28255-28274, 1997.

Talbot, R., Reactive nitrogen in Asian continental outflow over the western Pacific: results from the NASA TRACE-P airborne mission, *J. Geophys. Res.,* this issue.

People's Republic of China Yearbook (English edition) 2001**,** *China Yearbook Press, Beijing*,2001.

Trainer, M. *et al.* Correlation of ozone with NO_y in photochemically aged air. *J. Geophys. Res*., 98, 2917-2925, 1993.

Van Aardenne, J., Gregory. R. Carmichael, Hiram LevyII, David Streets, Leen Hordijk, Anthropogenic NO_x emissions in Asia in the period 1990–2020, *Atmospheric Environment*, Vol.33, 633-646, 1999.

Wang, C. J.-L., D. R. Blake, and F. S. Rowland, Seasonal variations in the atmospheric distribution of a reactive chorine compound, tetrachloraethene ($CCl_2=CCl_2$), *Geophys. Res. Lett.*, 22, 1097-1110, 1995.

Wang, T., K. S. Lam, L. Y. Chan, and A. S. Y. Lee, Trace gas measurements in coastal Hong Kong during the PEM-West B, *J. Geophys. Res.*, 102(D23), 28,575-28,588, 1997

Wang, T., Vincent T.F. Cheung, K. S. Lam, G. L. Kok, J.M. Harris, The characteristics

of ozone and related compounds in the boundary layer of the South China coast: temporal and vertical variations during autumn season, *Atmospheric Environment*, 35, 2735-2746, 2001.

Wang T., T. F. Cheung, and Y. S. Li, X. M.Yu and D. R. Blake, Emission characteristics of CO, NOx, SO$_2$ and indications of biomass burning observed at a rural site in eastern China, *J. Geophys. Res.*, 107, 10.1029/2001JD000724, 2002.

Whittlestone S., Radon measurements as an aid to the interpretation of atmospheric monitoring, *J. Atmos. Chem., 3*, 187-201, 1985.

Whittlestone, S., Zahorowski, W. Baseline radon detectors for shipboard use: development and deployment in the first Aerosol Characterization Experiment (ACE 1) , *J. Geophys. Res.*, 103(D13), 16,743-16,751, 1998.

Wilkniss, P. E., Larson, R. E., Bressan, D. J., and Steranka, J. Atmospheric Radon and continental dust near the antarctic and their correlation with air mass trajectories computed from nimbus 5 satellite photographs. *J. Appl. Meteorol.*, 13: 512-515, 1974.

Zahoroswski W. et al. Atmospheric radon-222 at three ACE-Asia sites: first year of observations, submitted to *J. Geophys. Res.*, 2002.

Figure captions

Figure 1   Geopotential height and streamlines over eastern Asia for (a) February 19-

April 30, 2002, (b) a case of cold front passage on February 28 and (c) a case

of maritime inflow on April 29.

(Plots are made using NCEP/NCAR reanalysis data available at

http://www.cdc.noaa.gov/cdc/data.ncep.renalysis.html)

Figure 2   Time series of ^{222}Rn, O_3, CO, NO, NO_y, SO_2, C_2H_4, C_2H_2, and CH_3Cl

measured at Hok Tsui and surface winds recorded at Waglan Island. Periods

for cold front passage (denoted by ▼), maritime air inflow (△) and

TRACE-P flights (✈) near Hong Kong are all marked.

Figure 3   Scatter plot of CO and ^{222}Rn

Figure 4   Time series of CO and ^{222}Rn during the passage of a cold front

Figure 5   Frequency distribution of wind direction for each air-mass group: Type M =

marine, Type C = continental, Type C-M = coastal, Type C-U = local urban

(see text for definition)

Figure 6   Scatter plot of O_3 and CO for the Type C, M, and C-M air mass groups

Figure 7   Scatter plots of O_3 and NO_y for the Type C, M, and C-M air mass groups

Figure 8   (a) Ozone versus $\Sigma RONO_2$ ($>C_2$) and (b) CO versus $\Sigma RONO_2$ ($>C_2$) (data

for all four air-mass groups are included.)

Figure 9   Scatter plot of SO_2 and NO_y for four air-mass groups

Figure 10   Scatter plot of CO and NO_y for four air-mass groups

Figure 11   Scatter plots of CO and selected NMHCs and halocarbons (data for all four

air-mass groups are included.)

Figure 12 Scatter plot of O_3, CO, SO_2, NO_y with C_2H_2/CO and C_3H_8/C_2H_6 (data for all

four air-mass groups are included.)

Figure 13 Frequency distributions of O_3, CO, SO_2 and NO_y during February 19-March
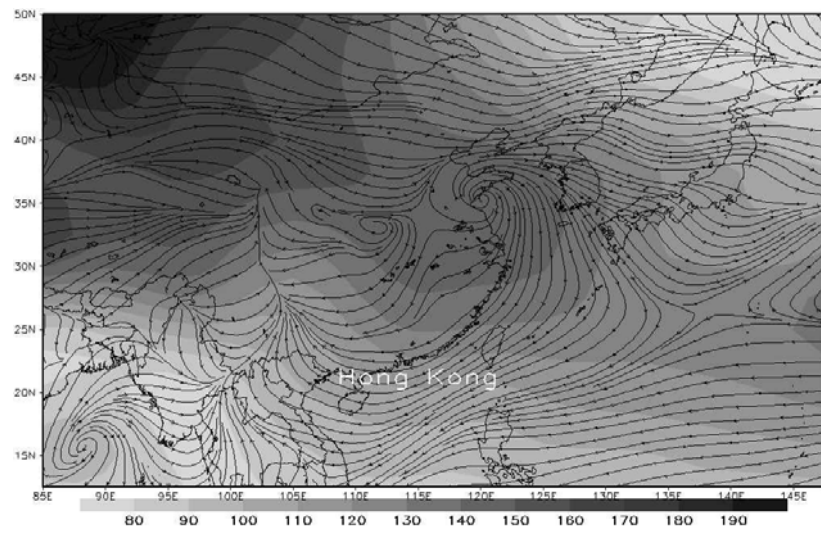
13 in 1994 and 2001

Figure 14 Difference in mean geopotential height for February 19-March 13 between

2001 (TRACE-P) and 1994 (PEM-WEST B)
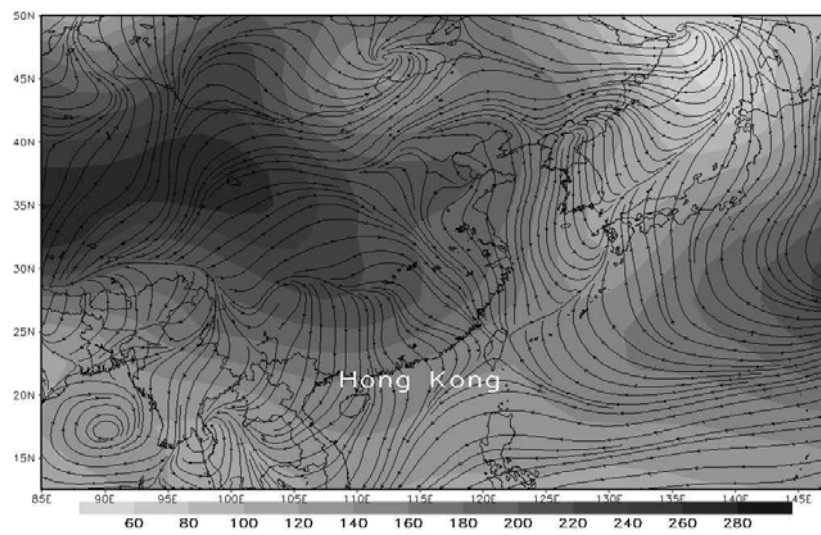
(Plots are made using NCEP/NCAR reanalysis data available at

http://www.cdc.noaa.gov/cdc/data.ncep.renalysis.html)

Figure 15 Wind roses for February 19-March 13 in 1994 (PEM-WEST B) and 2001

(TRACE-P)

Table captions

Table 1   Major synoptic patterns causing large day-to-day variations in trace gases

measured at Hok Tsui, Hong Kong

Table 2   Statistics of trace gases measured during February 19-April 30, 2001 at Hok

Tsui

Table 3   Statistics of principal trace gas species for each air-mass type: Type M =

marine, Type C-M = coastal, Type C = continental, Type C-U = local urban

Table 4   Comparison of O_3, CO, SO_2 and NO_y during February 19-March 13 in 1994

(PEM-WEST B) and 2001 (TRACE-P)

Table 5   Comparison of surface meteorological conditions during February

19-March 13 in 1994 (PEM-WEST B) and 2001 (TRACE-P)

(a)
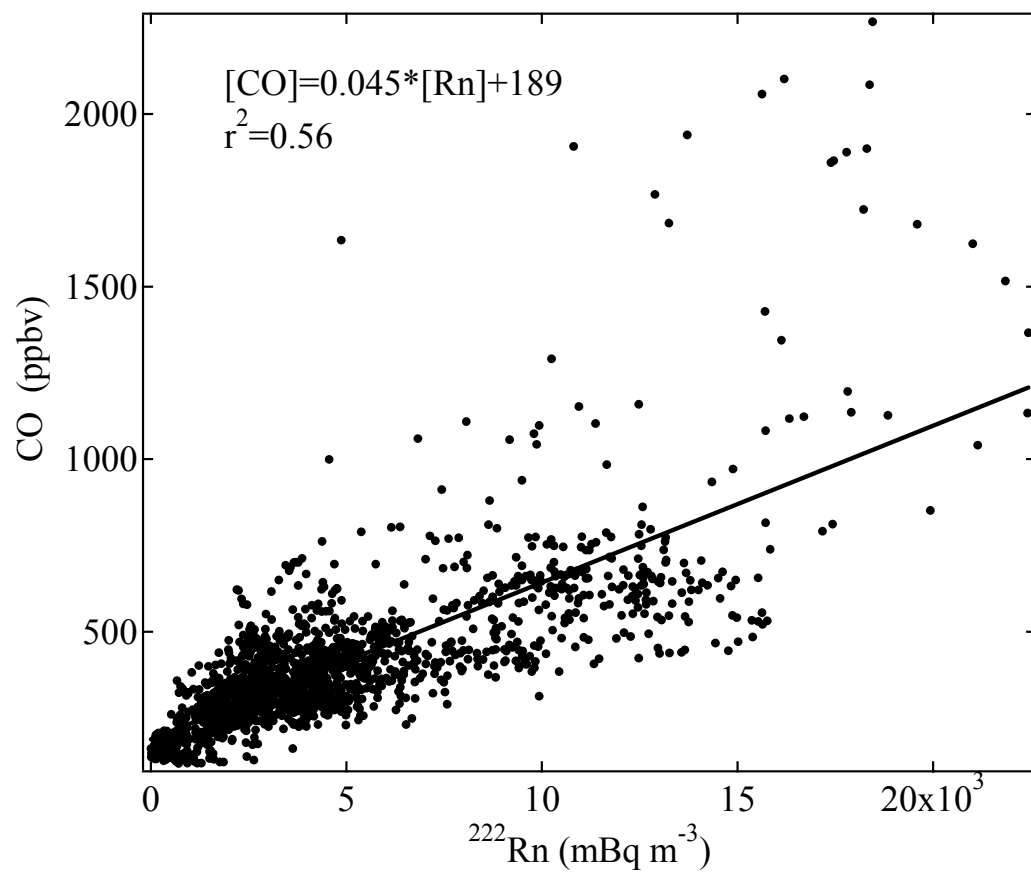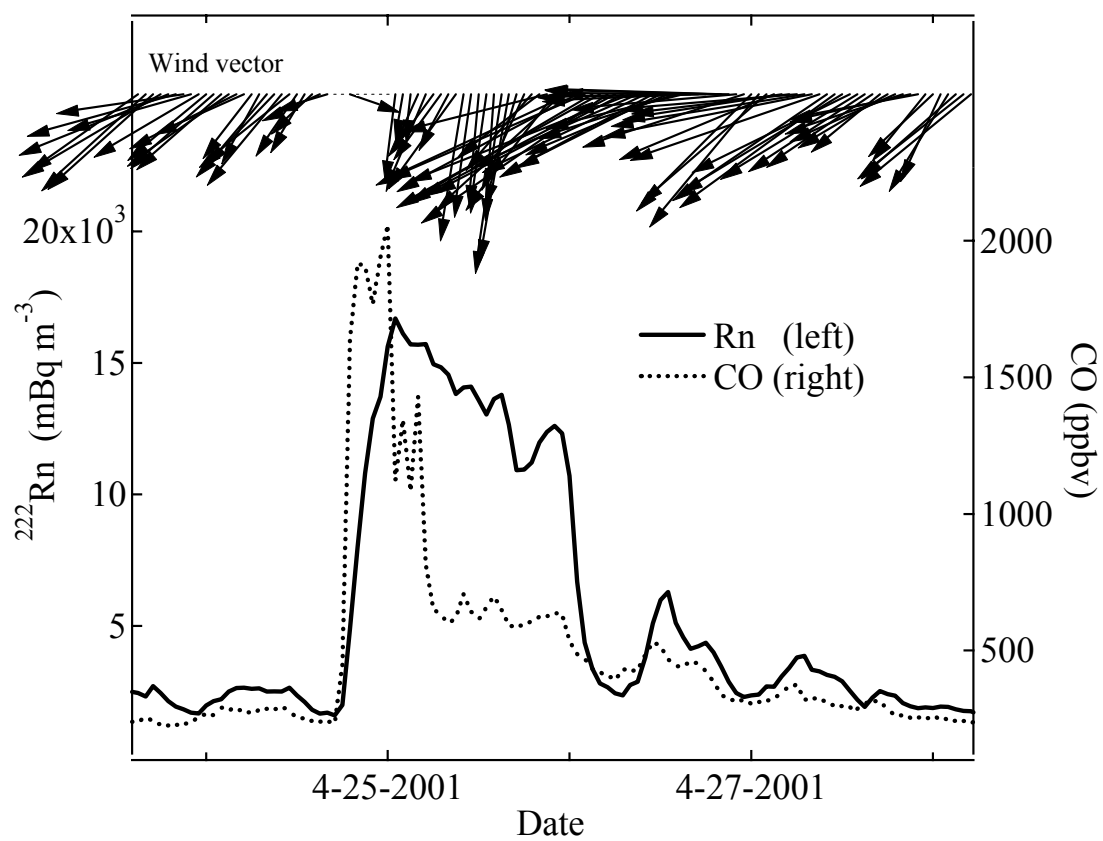

(b)
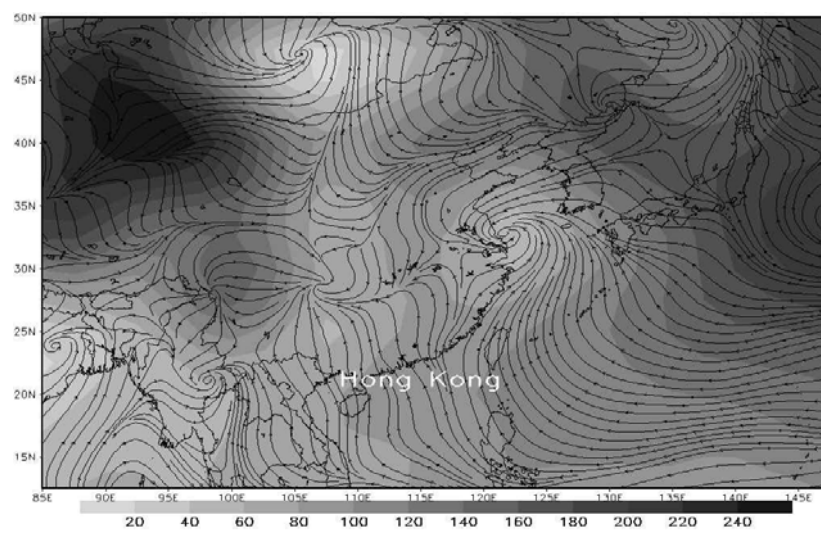
(c)

Figure 1
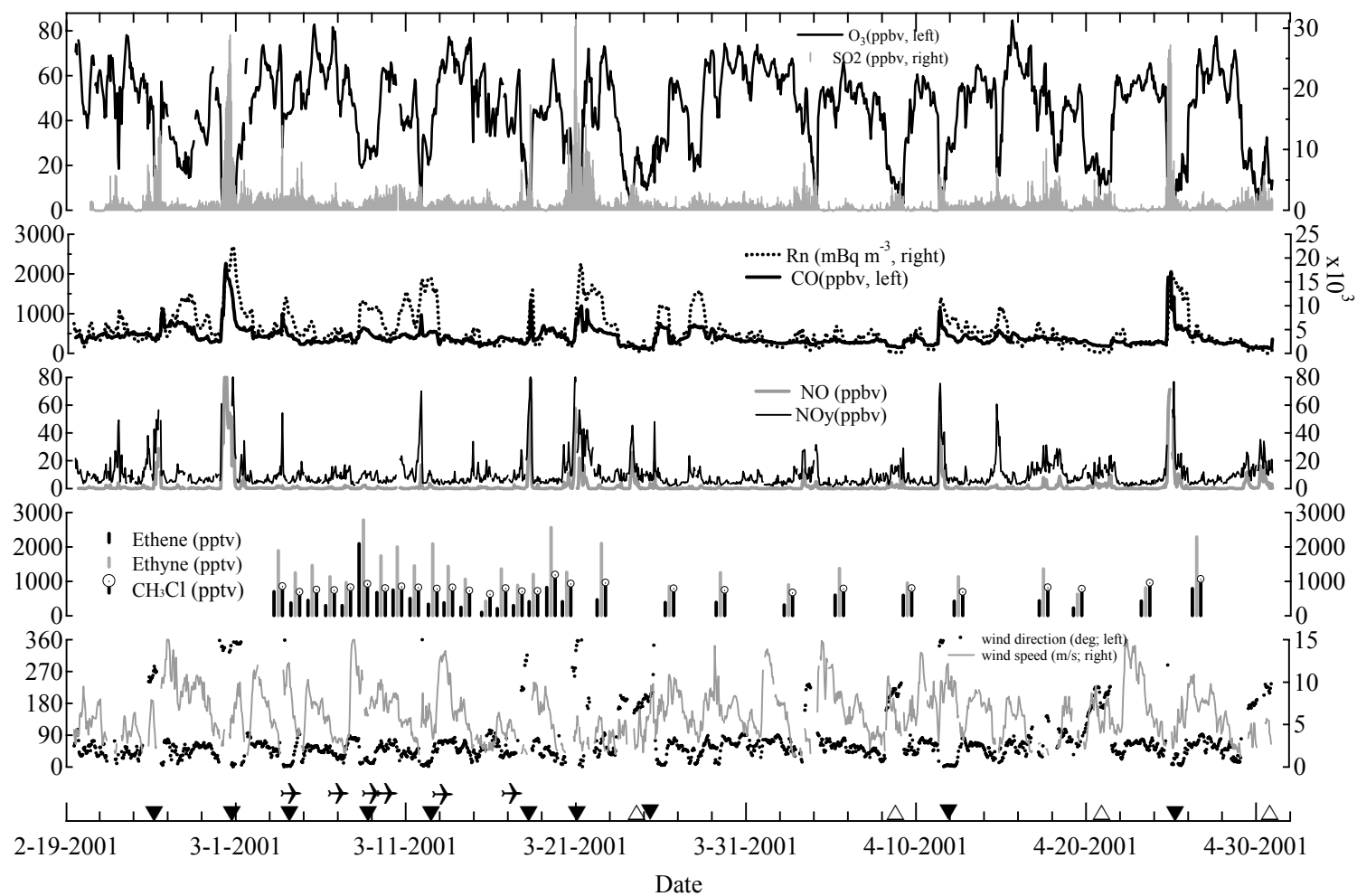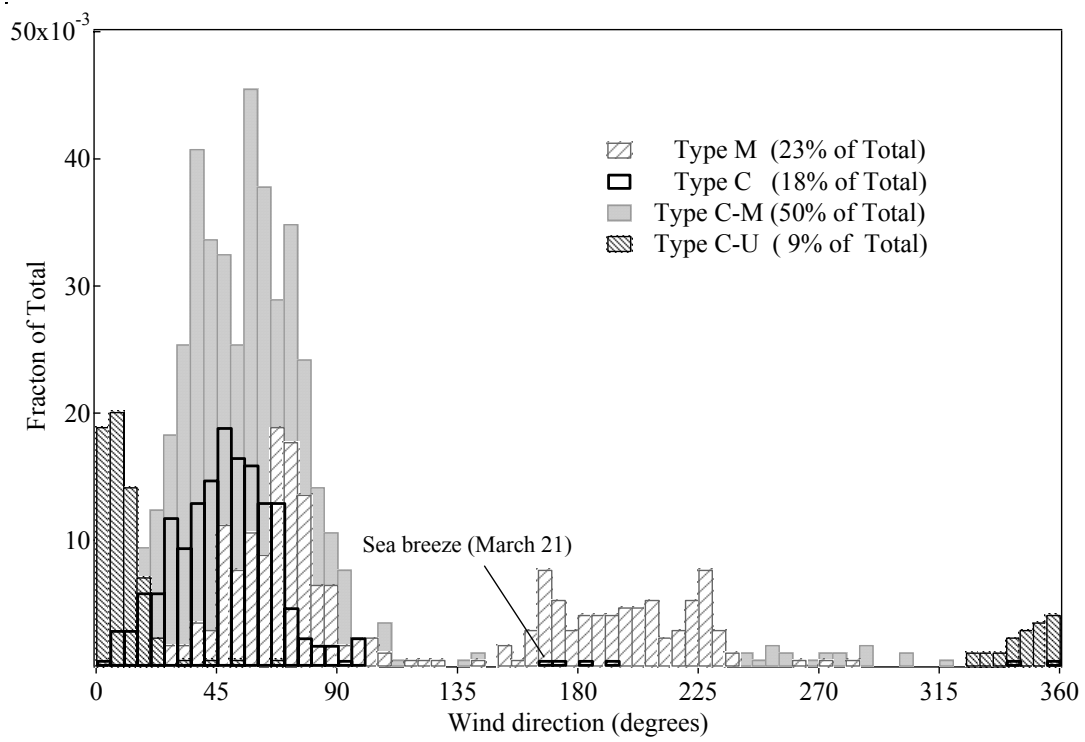
Figure 2

Figure 3

Figure 4

Figure 5

Type C $[O_3]=-0.04*[CO]+63.6$ $r^2=0.21$

Type C-M $[O_3]=0.003*[CO]+52.4$ $r^2=0.0006$

Type M $[O_3]=0.18*[CO]-5.7$ $r^2=0.4$

Figure 6

$[O_3] = -0.58*[NOy] + 48.4$
$r^2 = 0.13$

Type C

$[O_3] = -0.88*[NOy] + 61.0$
$r^2 = 0.24$

Type C-M

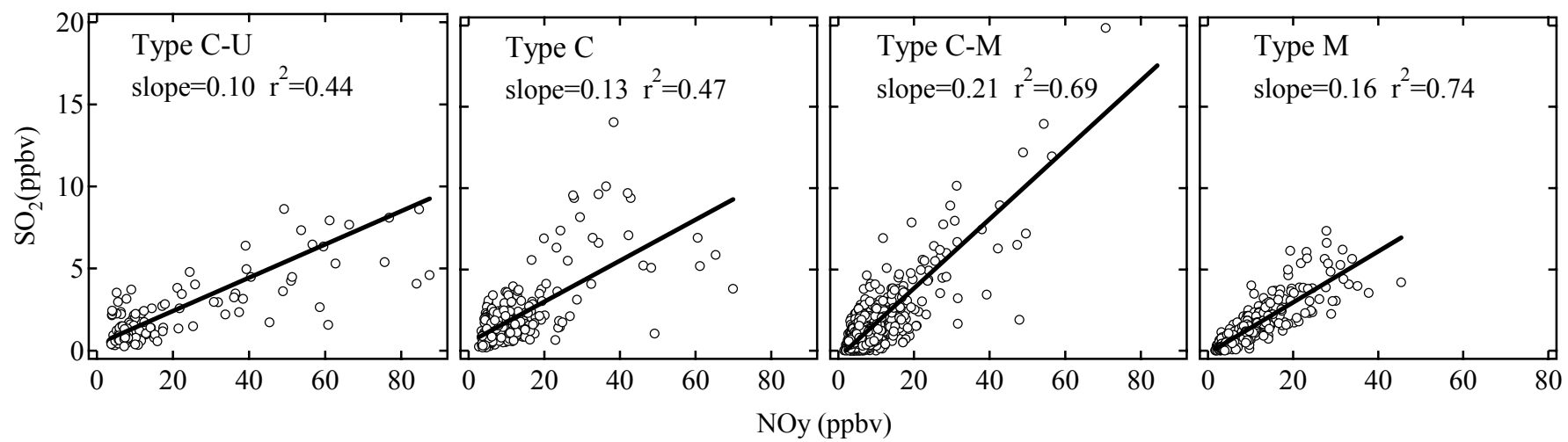$[O_3] = -1.74*[NOy] + 54.4$
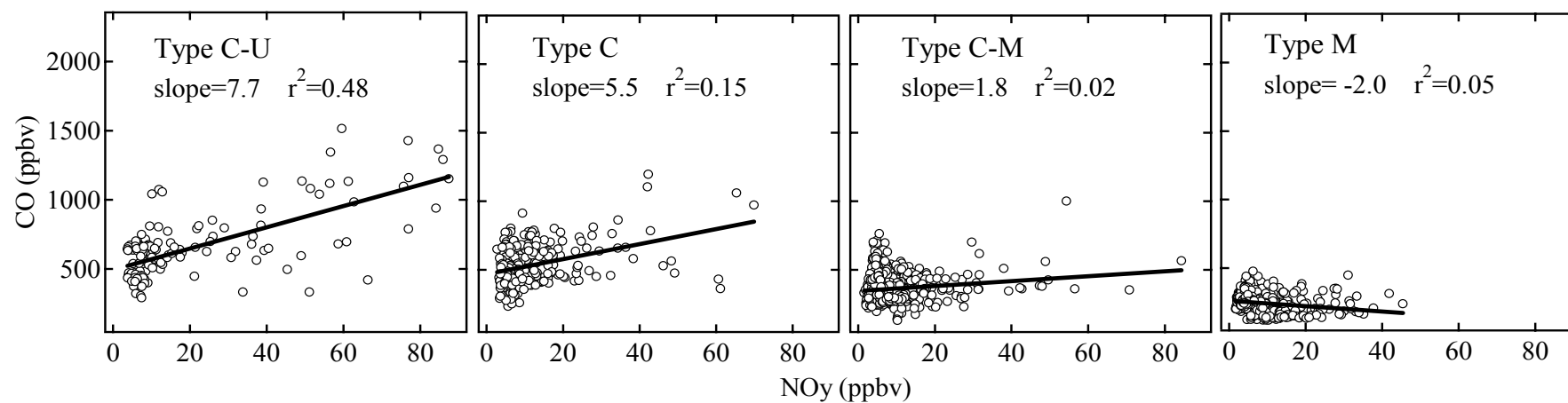$r^2 = 0.45$

Type M
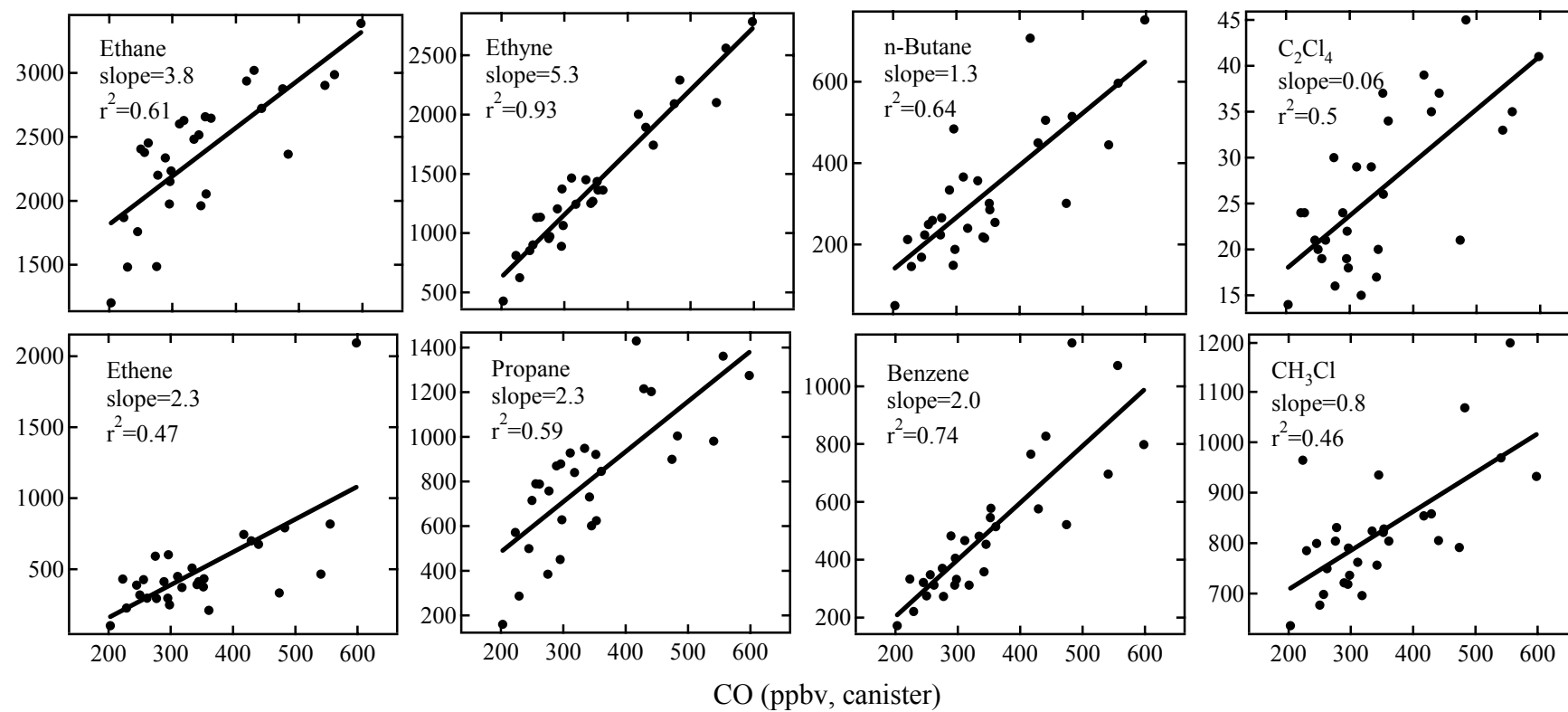
NOy (ppbv)

O_3 (ppbv)
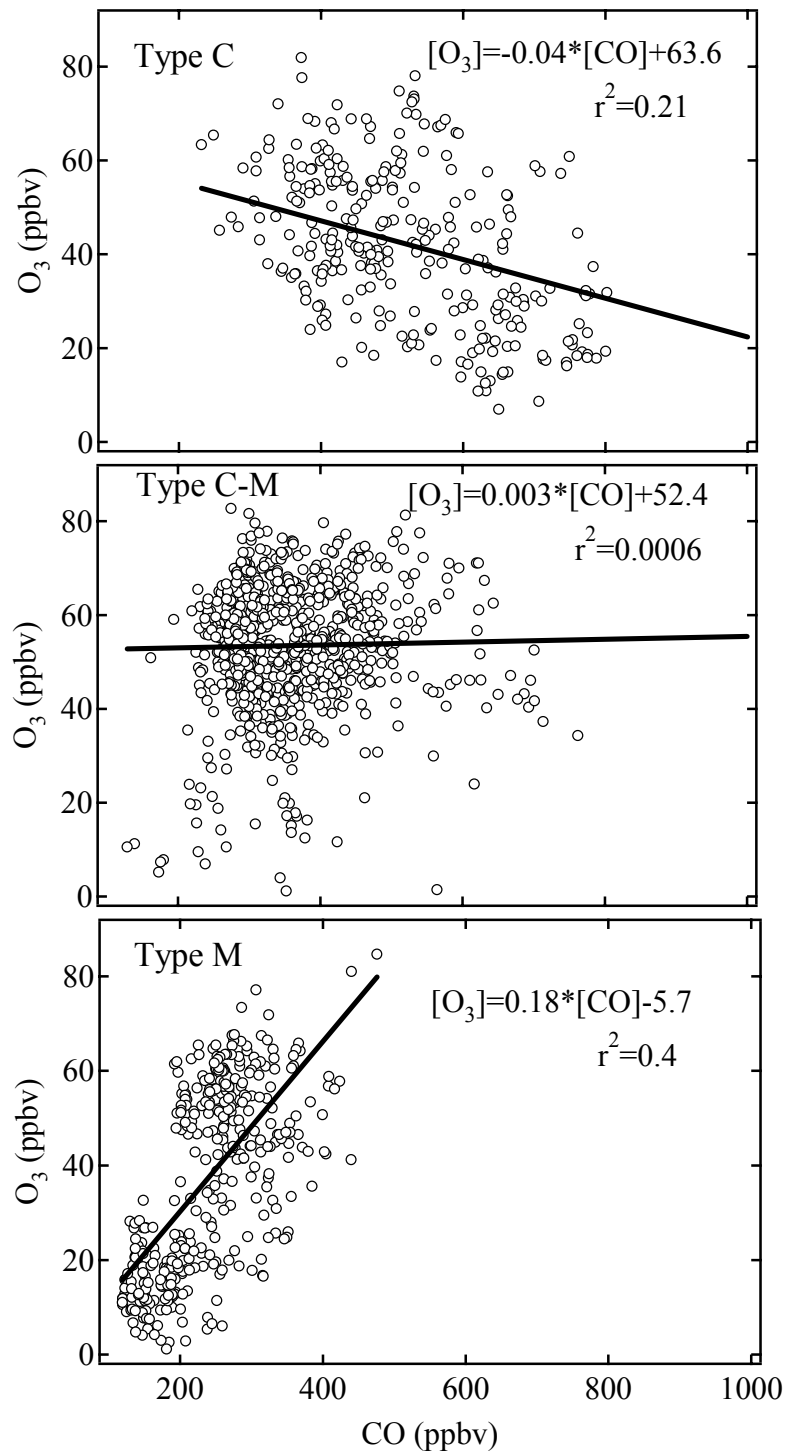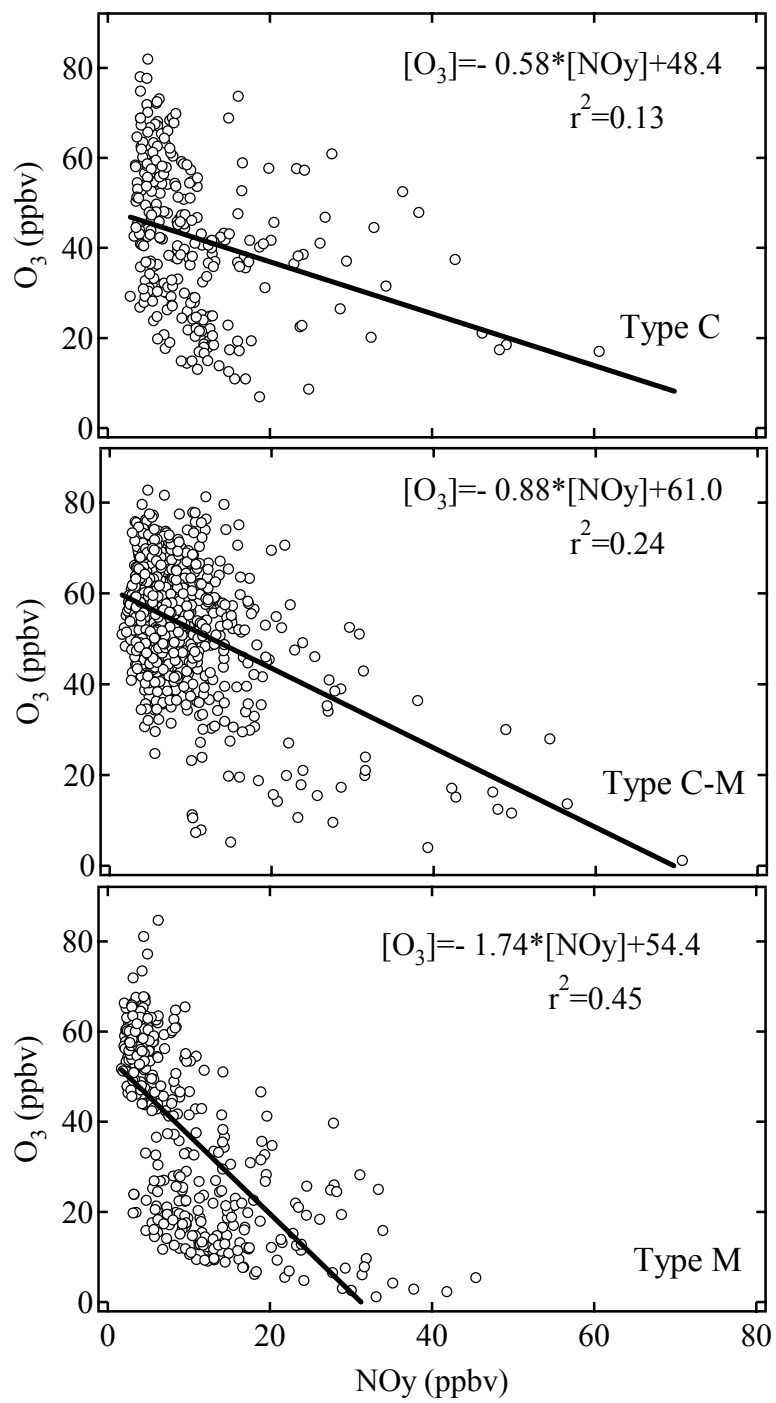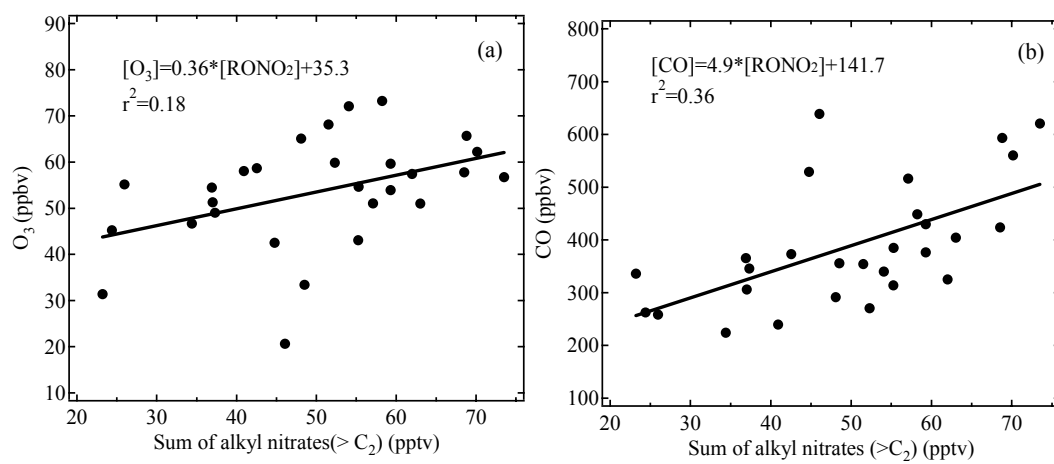
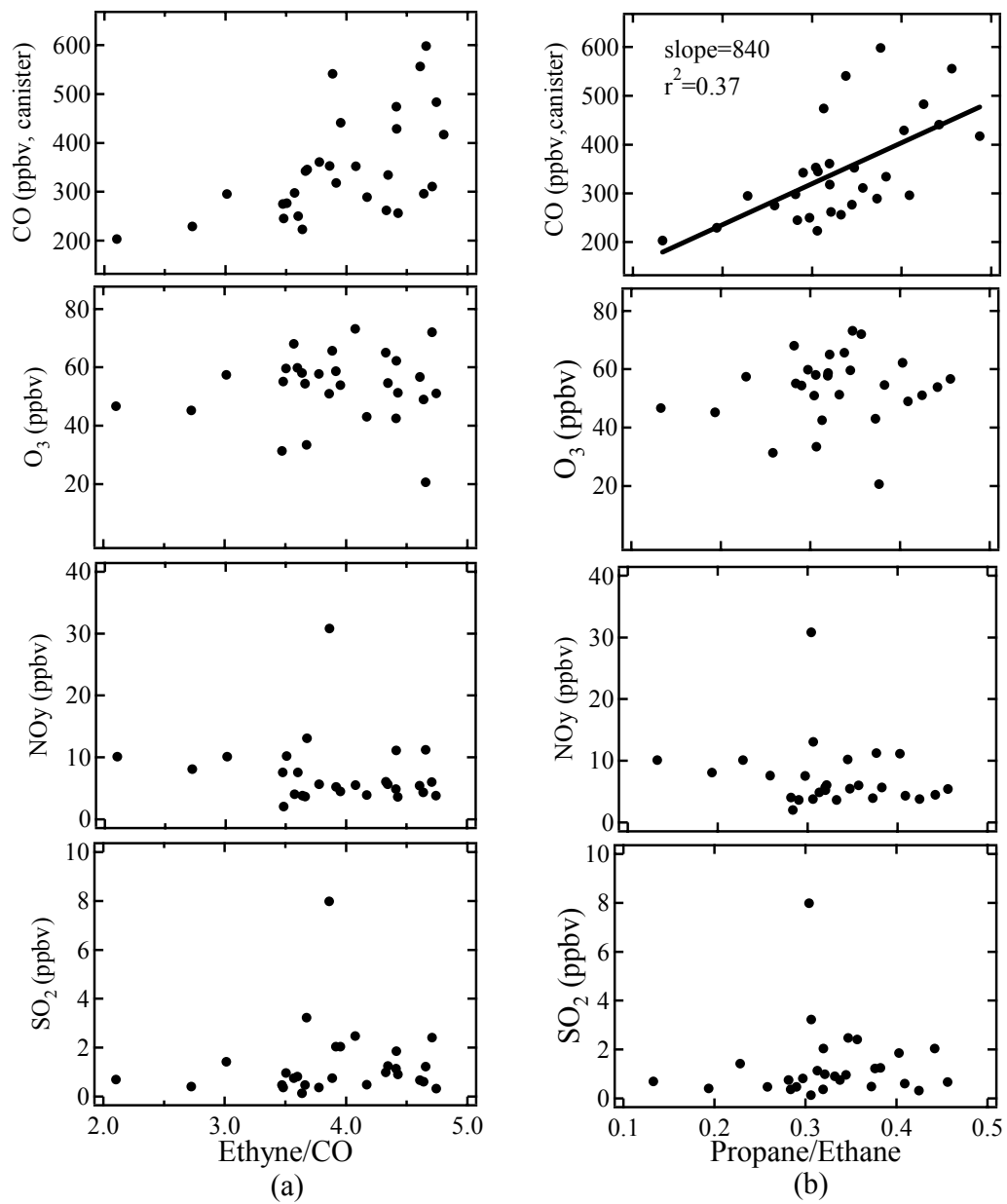Figure 7

Figure 8 (a) (b)

Figure 9

Figure 10
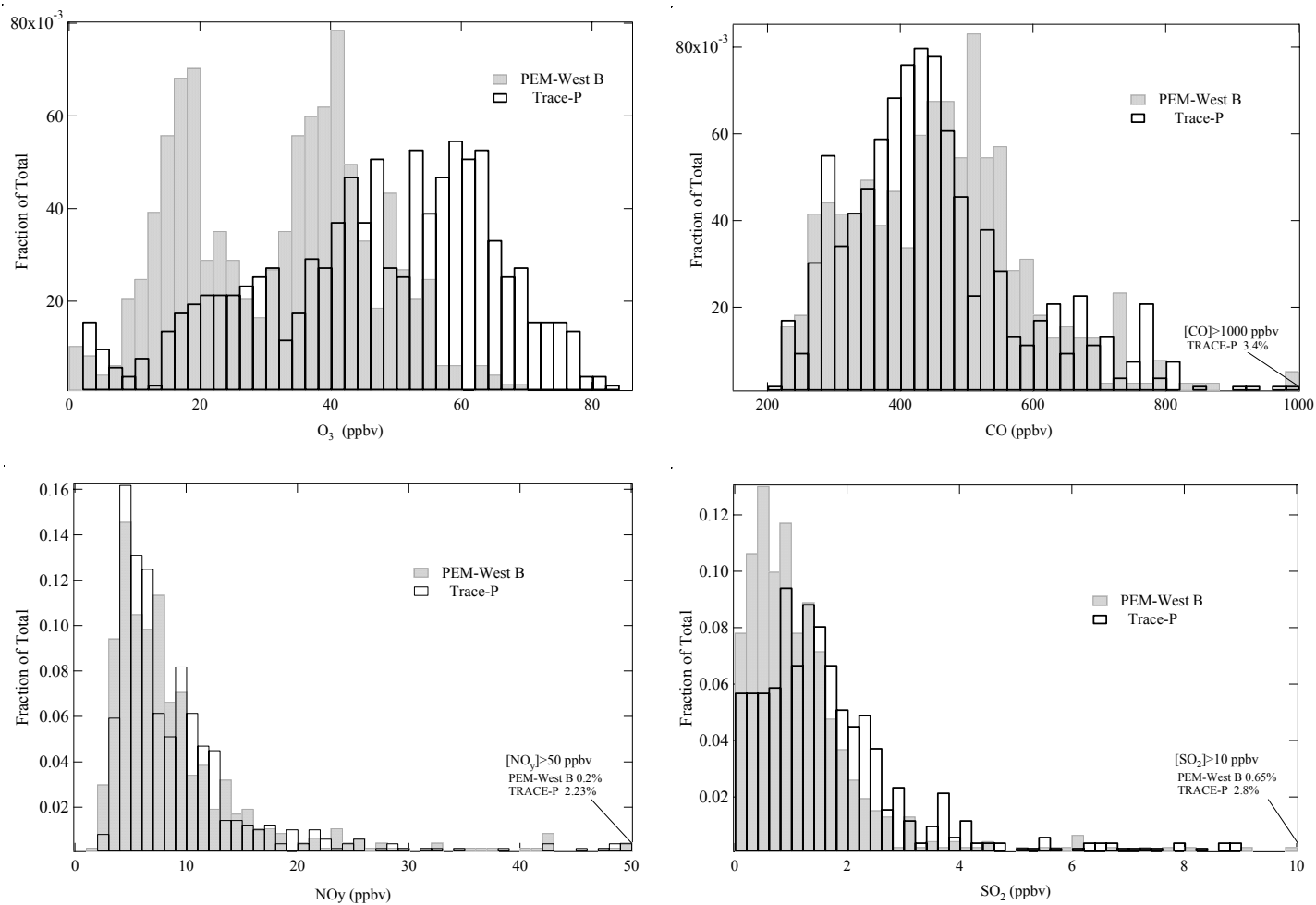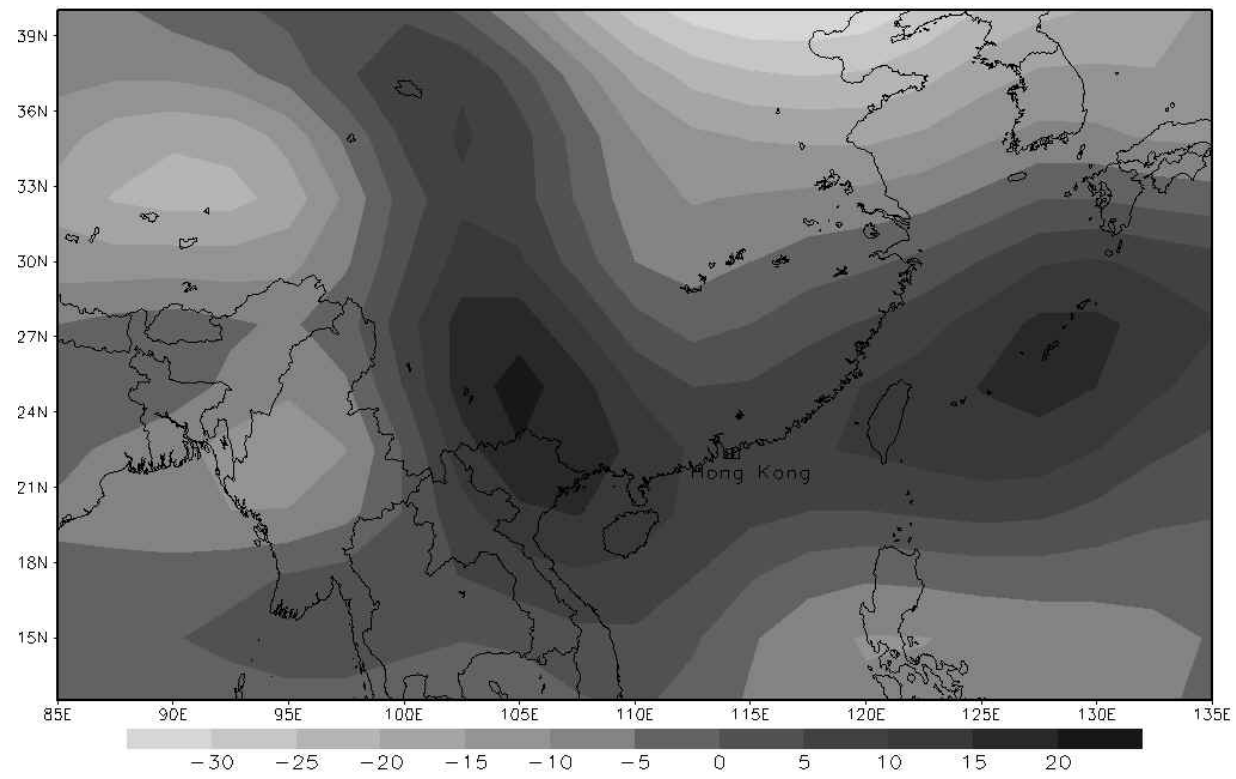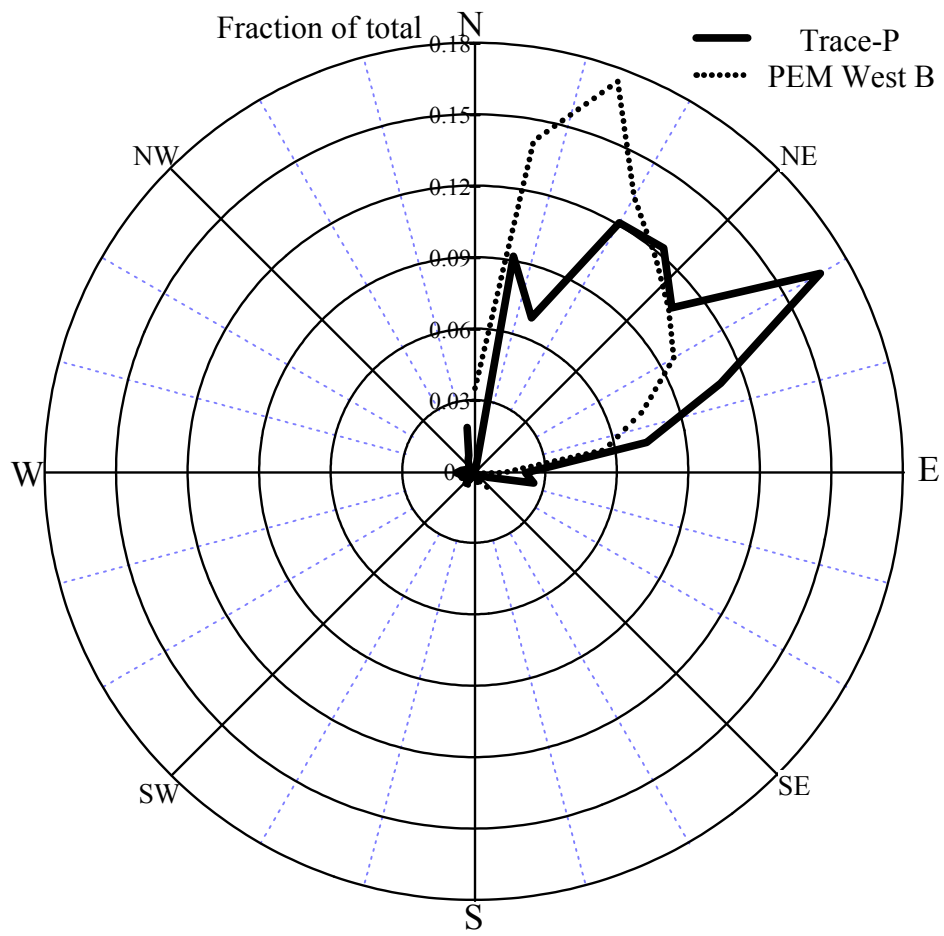
Figure 11

Figure 12

Figure 13

Figure 14

Figure 15

Table 1

Date	Main weather/synoptic conditions	Trace gas variations
Feb 24-25	A cold front arrived on Feb 24, which caused some rainfall (8.8mm) on Feb 25. The air temperature dropped by about 5℃ in the next two days.	The CO, SO_2 and NO_y levels increased sharply; but on Feb 25 even though the CO and ^{222}Rn remained at a relatively high level, SO2 and NO_y showed a significant decrease due to wet deposition.
Feb 28	A strong cold front swept over Hong Kong bringing in persistent W-NW winds for about 24 hours.	CO, SO_2, NO_y, ^{222}Rn reached very high levels; O_3 dropped to near zero due to chemical titration by fresh urban emissions.
March 3-4	A high-pressure system covered southern China with a strong (>10m/s) N-NE wind.	CO, NO_y and SO_2 increased moderately, but the O_3 level was relatively high (60-80 ppbv) in the next several days.
March 7-9	A cold front passed over Hong Kong from a northeasterly direction.	Trace gases showed a moderate increase; aerosol data revealed a sandstorm arriving in Hong Kong on March 9 associated with this cold front.
March 11-12	A cold front arrived	NO_y, ^{222}Rn and CO increased sharply with increasing O_3.
March 18	An intense high pressure moved to South China causing a surge of cold weather in Hong Kong.	CO, SO_2, NO and NO_y all increased sharply, while O_3 decreased; the very high ratio of NO to NO_y suggests fresh emissions from nearby urban areas.
March 20-21	A high-pressure system moved slowly from South China to Hong Kong bringing sunny conditions over Hong Kong; a sea-land breeze was observed.	CO, SO_2, NO_y, ^{222}Rn remained at high levels; the pollutants were re-circulated due to the sea breeze.
March 22-23	A sustained southerly air flow brought in marine air masses from the South China Sea.	O_3 and CO dropped to low levels, but NO, NO_y and SO_2 were present at high levels, possibly due to emissions from ships.
March 25	A cold front passed through Hong Kong.	The CO and ^{222}Rn showed moderate increases.
April.8	A weak cyclone located west of Hong Kong brought southerly winds for about one day.	O_3, CO, Rn, and some NMHCs were present at very low levels, again, the SO_2 and NO_y levels were moderately high due to emissions from ships.
April. 11-12	A cold font passed in the morning of April 11; Hong Kong experienced persistent strong northerly winds.	High levels of CO, SO_2 and NO_y were observed when the cold front arrived; The high NO/NO_y indicated fresh emissions.
Apr.20	The wind direction showed a clockwise shift, due to the activity of a strong low-pressure system over South China.	O_3 and CO decreased with winds coming from the south; SO_2 and NO_y were elevated.
April. 24-25	A cold front arrived in Hong Kong on April 24; northerly winds lasted for more than one day due to a strong high pressure over the Chinese mainland.	Very sharp peaks of CO, SO_2, Rn, NO and NO_y were associated with the cold front.
April 28-30	Southerly and southwesterly winds prevailed.	Rn, CO, and O_3 were at reduced levels; again, SO_2, NO, and NO_y were elevated.

Table 2

Species	Mean	s.d.	Median	Range
O_3	45	19	49	1-85
CO	404	228	352	119-2267
NO[a]	2.7	8.6	0.5	0-86
NO_y	10.4	10.7	7.0	1.5-87.5
SO_2	1.8	3.0	1.1	0-31.4
^{222}Rn	4740	3754	3648	6-22432
CH_4	1872	31	1866	1822-1948
Ethane	2368	508	2406	1203-3387
Ethene	498	355	414	103-2094
Ethyne	1402	574	1268	427-2785
Propane	814	307	840	160-1430
propene	61	46	46	18-214
n-butane	326	169	266	50-752
i-butane	221	117	182	39-489
n-pentane	85	48	71	19-237
Benzene	492	241	454	172-1150
Toluene	540	482	363	110-1781
Ethylbenzene	60	53	46	8-257
m-o-p-xylene	113	117	82	20.8-562.2
EthylChloride	19.1	9.4	17.5	9.8-48.5
$CHCl_3$	27.1	12.4	23.7	15.5-68.8
CCl_4	112.4	4.6	111.6	104.1-125.2
CH_2Cl_2	167.7	53.7	161.3	65.8-333.2
C_2HCl_3	22.0	33.2	13.1	5.2-176.2
CH_3Cl	821	120	803	636.4-1197.1
CH_3Br	12.4	1.8	11.6	10.4-17.9
CH_3I	2.07	0.66	2.04	0.81-3.45
CH_2Br_2	1.76	0.39	1.73	1.27-2.86
$CHBrCl_2$	0.55	0.11	0.54	0.38-0.89
$CHBr_3$	4.0	1.2	3.7	2.0-7.3
C_2Cl_4	26.3	8.6	23.8	13.8-44.6
$MeONO_2$	5.0	0.9	4.9	3.5-7.1
$EtONO_2$	5.8	1.3	5.8	3.9-8.5
i-$PrONO_2$	18.8	4.7	19.2	10.0-25.8
n-$PrONO_2$	2.05	0.51	2.1	1.2-3.0
2-$BuONO_2$	20.3	6.2	21.0	8.3-31.6
3-$PenONO_2$	4.5	1.6	4.4	1.5-7.7
2-$PenONO_2$	5.1	1.8	5.2	1.7-8.9
ΣRONO2（>C_2）	50.8	14.4	52.3	23.2-74.5

Units: O_3, CO, NO, NO_y and SO_2 and CH_4 are in ppbv; ^{222}Rn is in mBq m^{-3}, all others are in pptv.

[a] NO: 06:00~17:00 local time.

Table 3

Species	Type M		Type C-M		Type C		Type C-U	
	Mean	S.D.	Mean	S.D.	Mean	S.D.	Mean	S.D.
O_3	38	20	53	13	42	17	23	14
CO	242	70	362	105	540	189	766	424
NO	1.70	3.33	0.70	3.26	1.64	7.09	10.88	19.69
NO_y	9.74	7.70	8.46	7.51	11.63	10.37	21.19	22.32
SO_2	1.3	1.3	1.4	2.0	2.0	2.3	4.3	6.8
Ethane	1937	722	2195	481	2613	222	3387	-
Ethene	243	158	431	181	507	158	2094	-
Ethyne	1019	515	1202	509	1635	425	2785	-
Propane	535	347	721	303	966	198	1275	-
Propene	45	32	67	49	46	14	202	-
n-Butane	173	108	283	136	385	147	752	-
i-Butane	128	77	186	94	267	110	477	-
n-Pentane	62	42	78	52	93	39	179	-
Benzene	380	183	423	219	583	254	798	-
Toluene	225	104	455	364	631	545	1683	-
Ethylbenzene	27	17	48	30	65	46	257	-
CCl_4	114	4.5	112	5	112	4.4	117	-
CH_3Cl	792	150	826	127	813	115	932	-
CH_3Br	12.7	1.2	12.6	2.3	12.1	1.6	12	-
CH_3I	2.2	0.5	2.3	0.5	1.8	0.8	1.7	-
Ethyl Chloride	17	7	20	12	18	6	19	-
C_2Cl_4	23	10	25	7	28	10	41	-
C_3H_8/C_2H_6	0.25	0.10	0.32	0.07	0.37	0.06	0.38	-
C_2H_2/CO	3.2	0.9	3.8	0.6	4.3	0.4	4.7	-

Units: same as in Table 2.

For NHMCs and halons, the number of data points is 3, 14, 11 and 1 for Type M, Type C-M, Type-C and Type C-U, respectively.

Table 4

Species	Period	Mean	Median	10%	90%
O_3	PEM-WEST B	32	34	13	50
	TRACE-P	47	48	20	68
CO	PEM-WEST B	462	462	290	633
	TRACE-P	495	437	296	702
SO_2	PEM-WEST B	1.31	0.95	0.23	2.40
	TRACE-P	2.20	1.43	0.35	3.95
NO_y	PEM-WEST B	9.6	7.25	3.82	17.36
	TRACE-P	10.7	7.25	4.12	18.57

Table 5

Item	Unit	PEM West B (1994)	TRACE-P (2001)
Mean surface pressure [a]	hPa	1016.7	1017.4
Mean air temperature [a]	℃	15.3	17.9
Mean relative humidity [a]	%	84	77
Total Rainfall [a]	mm	15	6
Mean daily hours of sunshine [b]	Hr	1.8	5.1
Mean cloud cover fraction [b]*	--	6.7/8	4.8/8

[a]Data recorded at Waglan Island;

[b]Data recorded at King's Park

* Only data of local time 07:00 ~ 17:00 were used in the statistics.